

Axial-Flexural-Shear Coupled Vibration Analysis of Timoshenko Composite Beam Using Spectral Element Method

Piyush Rajput



Department of Civil Engineering
National Institute of Technology Rourkela
Sundargarh, Odisha, India – 769 008

Axial-Flexural-Shear Coupled Vibration Analysis of Timoshenko Composite Beam Using Spectral Element Method

A Thesis submitted in partial fulfillment of
the requirements for the award of the degree of

*Master of Technology in
Structural Engineering*

*Submitted to
National Institute of Technology Rourkela*

by

Piyush Rajput

(Roll No. 214CE2060)

under the supervision of

Prof. Manoranjan Barik



Department of Civil Engineering
National Institute of Technology Rourkela
Sundargarh, Odisha, India – 769 008

Dedicated to
The Almighty God
&
My Family
whose blessings have made
this thesis a reality...



Department of Civil Engineering
National Institute of Technology Rourkela
Rourkela-769 008 , Odisha , India. www.nitrkl.ac.in

Dr. Manoranjan Barik
Associate Professor

May , 2016

Certificate

This is to certify that the work in the thesis entitled *Axial-Flexural-Shear Coupled Vibration Analysis of Timoshenko Composite Beam Using Spectral Element Method* by *Piyush Rajput*, bearing Roll Number 214CE2060, is a record of an original research work carried out by him under my supervision and guidance in partial fulfillment of the requirements for the award of the degree of *Master of Technology* in *Structural Engineering, Department of Civil Engineering*. Neither this thesis nor any part of it has been submitted for any degree or academic award elsewhere.

Manoranjan Barik

Acknowledgement

Firstly, I would like to convey my heartily thanks and gratitude to my beloved guide, Prof. Manoranjan Barik, (Dept. of Civil Engineering, NIT, Rourkela) for his continuous guidance and support, with the help of which I have successfully been able to complete my research work.

I would like to acknowledge my special thanks to the Head of the Department, Prof. S.K. Sahu and all the faculty members of the Department of Civil Engineering, for providing me the deep insight and discernments given through the various course they had taught and also for their valuable guidance during my work.

I am also thankful to all my well wishers and the staff of Civil Engineering Department whose timely help and co-operation allowed me to complete my research work in time and bring out this thesis. My special thanks to PhD Scholars *Biraja Prasad Mishra, Saleema Panda* and my classmate *Praveen Kumar Sahu*.

Last, but not the least, I would like to profound my deepest gratitude to my mother *Dr. R.R. Rajput* for her exceptional love and encouragement throughout this entire journey, without whom I would have struggled to find the inspiration and motivation needed to complete this thesis.

Piyush Rajput

Roll No. 214CE2060

Structural Engineering

Abstract

The free vibration analysis of an axial-flexural-shear coupled composite beam with different boundary conditions has been studied by many researchers using various computational methods of analysis such as Finite Element Method (FEM), Differential Transformation Element Method (DTEM), Quadrature Element Method (QEM), Differential Quadrature Element Method (DQEM) etc., besides the traditional mathematical methods and exact methods. In this study the Spectral Element Method (SEM) for analysis of free vibration of both symmetrical as well as asymmetrical composite beam with various boundary conditions is presented considering the effects of axial, bending and shear deformations. Initially, spectral element matrices in the time domain are derived for axial-bending-shear coupled vibration from the governing differential equations of motion by using Hamilton principle and after that, it has been transformed into the frequency domain.

With the consideration of least number of elements the higher accuracy in the natural frequencies is possible using SEM, thus proving that this method is highly accurate and having very high computational efficiency. So to confirm the validity of this method several numerical examples are presented and the results are then compared with the other existing solutions.

Keywords: Spectral Element Method (SEM); Analytical methods; Exact methods; Axial-Bending-Shear coupling; Timoshenko composite beam; Finite Element Method (FEM)

Contents

| | |
|---|-------------|
| Certificate | iii |
| Acknowledgement | iv |
| Abstract | v |
| Abbreviation | ix |
| List of Figures | xi |
| List of Tables | xiii |
| 1 Introduction | 1 |
| 1.1 Finite Element Method | 2 |
| 1.2 Dynamic Stiffness Method | 2 |
| 1.3 Spectral Analysis Method | 3 |
| 1.4 Spectral Element Method | 4 |
| 1.5 Objectives | 5 |
| 2 Literature Review | 6 |
| 3 Spectral Element model for Composite Timoshenko Beam | 10 |
| 3.1 Spectral Element Methodology | 10 |
| 3.2 Theory of Composite Mechanics | 11 |

| | | |
|----------|---|-----------|
| 3.2.1 | Three-Dimensional Stress Strain Relationship | 11 |
| 3.2.2 | Stress-Strain Relationships for an Orthotropic Lamina | 12 |
| 3.2.3 | Strain-Displacement Relationships | 15 |
| 3.2.4 | Resultant Forces and Moments | 16 |
| 3.3 | Equations of Motion for Symmetrical Composite Laminated Beams | 18 |
| 3.4 | Equations of Motion for Non Symmetrical Composite Laminated Beams | 23 |
| 3.5 | Dynamics of Axial-Bending-Shear Coupled Composite Beams | 29 |
| 3.5.1 | Equation of Motion | 29 |
| 3.5.2 | Spectral Element Modeling | 30 |
| 3.5.2.1 | Formulation of Governing equations of motion in frequency domain | 30 |
| 3.5.2.2 | Spectral Nodal DOFs, Forces, and Moments | 31 |
| 3.5.2.3 | Dynamic shape functions | 32 |
| 3.5.2.4 | Weak Form of frequency domain Governing Equations | 36 |
| 3.5.2.5 | Formulation of Spectral Element Equation | 37 |
| 3.5.3 | Spectral Element Analysis | 39 |
| 4 | Numerical Results and Discussion | 41 |
| 4.1 | Natural frequencies of a symmetrical laminated composite beam with different boundary conditions | 41 |
| 4.1.1 | $[0^\circ/90^\circ/90^\circ/0^\circ]$ Ply Oriented Beam | 43 |
| 4.1.2 | $[+15^\circ/-15^\circ/-15^\circ/+15^\circ]$ Ply Oriented Beam | 49 |
| 4.1.3 | $[+30^\circ/-30^\circ/-30^\circ/+30^\circ]$ Ply Oriented Beam | 55 |
| 4.1.4 | $[+45^\circ/-45^\circ/-45^\circ/+45^\circ]$ Ply Oriented Beam | 61 |
| 4.2 | Natural frequencies of a asymmetrical laminated composite beam with different boundary conditions | 67 |
| 4.2.1 | $[0^\circ/90^\circ/0^\circ/90^\circ]$ Ply Oriented Beam | 68 |

| | | |
|----------|---|-----------|
| 4.3 | Effect of Coupling Rigidity and Axial Force on dispersion curve . . | 74 |
| 5 | Conclusion | 81 |
| 6 | Future scope of study | 83 |

Abbreviations

| | |
|------------------------|--|
| E | Young's modulus |
| G | Shear modulus |
| κ | Shear correction factor (depend upon the shape of the cross section) |
| A | Cross-sectional area |
| I | Area moment of inertia about neutral axis |
| L | Length of the beam |
| $N(x, t)$ | Axial Force |
| $M(x, t)$ | Bending Moment |
| $Q(x, t)$ | Transverse shear force |
| $u_0(x, t)$ | Axial displacement |
| $w_0(x, t)$ | Bending displacement |
| $w(x, t)$ | Transverse displacement |
| $\theta(x, t)$ | Slope due to bending respectively |
| EA | Axial rigidity |
| EI | Flexural rigidity |
| K | Coupling rigidity |
| κGA | Apparent shear rigidity |
| \bar{Q}_1, \bar{Q}_5 | Transformed reduced stiffnesses |
| c_1, c_2, c_3 | Damping coefficient |
| T | Kinetic energy |
| U | Strain energy |

| | |
|----------------------------|---|
| δW | Virtual work done |
| ρ | Mass density |
| ρA | Apparent mass of the beam |
| ρR | Apparent first order mass moment of inertia about the y-axis |
| ρI | Apparent second order mass moment of inertia about the y-axis |
| $N_{r1}(t), N_{r2}(t)$ | Axial forces |
| $M_{r1}(t), M_{r2}(t)$ | Bending moments |
| $Q_{r1}(t), Q_{r2}(t)$ | Transverse forces |
| ω_n | Discrete frequency |
| f_q | Nyquist frequency |
| $k_p (p = 1, 2, \dots, 6)$ | Six wavenumber |
| α | Constant |
| β | Constant |
| N_w, N_u, N_θ | Dynamic shape function |
| δd | Virtual displacement |
| f_c | External force |
| f_d | Internal force |
| $S(\omega)$ | Spectral element matrix |
| $S_g(\omega)$ | Global dynamic stiffness matrix or global spectral matrix |
| d_g | Global spectral nodal DOFs vector |
| f_g | Global spectral nodal forces vector |

List of Figures

| | | |
|-----|---|----|
| 3.1 | The global and local coordinate systems for a composite laminated beam | 13 |
| 3.2 | Geometry of an N-layered laminate | 17 |
| 3.3 | Sign convention for the Timoshenko-beam element | 21 |
| 3.4 | Sign convention and boundary forces for composite Timoshenko beam element | 26 |
| 3.5 | Spectral nodal DOFs and forces for composite Timoshenko beam element | 26 |
| 4.1 | Symmetrical cross-ply orientation $[0^\circ/90^\circ/90^\circ/0^\circ]$ | 43 |
| 4.2 | Symmetrical cross-ply orientation $[+15^\circ/-15^\circ/-15^\circ/+15^\circ]$. . . | 49 |
| 4.3 | Symmetrical cross-ply orientation $[+30^\circ/-30^\circ/-30^\circ/+30^\circ]$. . . | 55 |
| 4.4 | Symmetrical cross-ply orientation $[+45^\circ/-45^\circ/-45^\circ/+45^\circ]$. . . | 61 |
| 4.5 | Asymmetrical cross-ply orientation $[0^\circ/90^\circ/0^\circ/90^\circ]$ | 68 |
| 4.6 | Variation of Non-Dimensional Natural Frequency in dispersion curve with varying coupling rigidity K in axial mode | 75 |
| 4.7 | Variation of Non-Dimensional Natural Frequency in dispersion curve with varying coupling rigidity K in bending mode | 76 |
| 4.8 | Variation of Non-Dimensional Natural Frequency in dispersion curve with varying coupling rigidity K in shear mode | 77 |
| 4.9 | Variation of Non-Dimensional Natural Frequency in dispersion curve with varying axial loading P in axial mode | 78 |

| | | |
|------|---|----|
| 4.10 | Variation of Non-Dimensional Natural Frequency in dispersion curve with varying axial loading P in bending mode | 79 |
| 4.11 | Variation of Non-Dimensional Natural Frequency in dispersion curve with varying axial loading P in shear mode | 80 |

List of Tables

| | | |
|-----|---|----|
| 4.1 | Comparison of non-dimensional natural frequencies for a symmetrical $[0^\circ/90^\circ/90^\circ/0^\circ]$ angle-ply simply supported composite beam | 44 |
| 4.2 | Comparison of non-dimensional natural frequencies for a symmetrical $[0^\circ/90^\circ/90^\circ/0^\circ]$ angle-ply cantilevered composite beam | 45 |
| 4.3 | Comparison of non-dimensional natural frequencies for a symmetrical $[0^\circ/90^\circ/90^\circ/0^\circ]$ angle-ply clamped-clamped composite beam | 46 |
| 4.4 | Comparison of non-dimensional natural frequencies for a symmetrical $[0^\circ/90^\circ/90^\circ/0^\circ]$ angle-ply clamped-simply supported composite beam | 47 |
| 4.5 | Comparison of non-dimensional natural frequencies for a symmetrical $[0^\circ/90^\circ/90^\circ/0^\circ]$ angle-ply free-free composite beam | 48 |
| 4.6 | Comparison of non-dimensional natural frequencies for a symmetrical $[+15^\circ/-15^\circ/-15^\circ/+15^\circ]$ angle-ply simply supported composite beam | 50 |
| 4.7 | Comparison of non-dimensional natural frequencies for a symmetrical $[+15^\circ/-15^\circ/-15^\circ/+15^\circ]$ angle-ply cantilevered composite beam | 51 |

| | | |
|------|---|----|
| 4.8 | Comparison of non-dimensional natural frequencies for a symmetrical $[+15^\circ / -15^\circ / -15^\circ / +15^\circ]$ angle-ply clamped-clamped composite beam | 52 |
| 4.9 | Comparison of non-dimensional natural frequencies for a symmetrical $[+15^\circ / -15^\circ / -15^\circ / +15^\circ]$ angle-ply clamped-simply supported composite beam | 53 |
| 4.10 | Comparison of non-dimensional natural frequencies for a symmetrical $[+15^\circ / -15^\circ / -15^\circ / +15^\circ]$ angle-ply free-free composite beam | 54 |
| 4.11 | Comparison of non-dimensional natural frequencies for a symmetrical $[+30^\circ / -30^\circ / -30^\circ / +30^\circ]$ angle-ply simply supported composite beam | 56 |
| 4.12 | Comparison of non-dimensional natural frequencies for a symmetrical $[+30^\circ / -30^\circ / -30^\circ / +30^\circ]$ angle-ply cantilevered composite beam | 57 |
| 4.13 | Comparison of non-dimensional natural frequencies for a symmetrical $[+30^\circ / -30^\circ / -30^\circ / +30^\circ]$ angle-ply clamped-clamped composite beam | 58 |
| 4.14 | Comparison of non-dimensional natural frequencies for a symmetrical $[+30^\circ / -30^\circ / -30^\circ / +30^\circ]$ angle-ply clamped-simply supported composite beam | 59 |
| 4.15 | Comparison of non-dimensional natural frequencies for a symmetrical $[+30^\circ / -30^\circ / -30^\circ / +30^\circ]$ angle-ply free-free composite beam | 60 |
| 4.16 | Comparison of non-dimensional natural frequencies for a symmetrical $[+45^\circ / -45^\circ / -45^\circ / +45^\circ]$ angle-ply simply supported composite beam | 62 |

| | |
|--|----|
| 4.17 Comparison of non-dimensional natural frequencies for a symmetrical $[+45^\circ / -45^\circ / -45^\circ / +45^\circ]$ angle-ply cantilevered composite beam | 63 |
| 4.18 Comparison of non-dimensional natural frequencies for a symmetrical $[+45^\circ / -45^\circ / -45^\circ / +45^\circ]$ angle-ply clamped-clamped composite beam | 64 |
| 4.19 Comparison of non-dimensional natural frequencies for a symmetrical $[+45^\circ / -45^\circ / -45^\circ / +45^\circ]$ angle-ply clamped-simply supported composite beam | 65 |
| 4.20 Comparison of non-dimensional natural frequencies for a symmetrical $[+45^\circ / -45^\circ / -45^\circ / +45^\circ]$ angle-ply free-free composite beam | 66 |
| 4.21 Comparison of non-dimensional natural frequencies for a asymmetrical $[0^\circ / 90^\circ / 0^\circ / 90^\circ]$ angle-ply simply supported composite beam | 69 |
| 4.22 Comparison of non-dimensional natural frequencies for a asymmetrical $[0^\circ / 90^\circ / 0^\circ / 90^\circ]$ angle-ply cantilevered composite beam | 70 |
| 4.23 Comparison of non-dimensional natural frequencies for a asymmetrical $[0^\circ / 90^\circ / 0^\circ / 90^\circ]$ angle-ply clamped-clamped composite beam | 71 |
| 4.24 Comparison of non-dimensional natural frequencies for a asymmetrical $[0^\circ / 90^\circ / 0^\circ / 90^\circ]$ angle-ply clamped-simply supported composite beam | 72 |
| 4.25 Comparison of non-dimensional natural frequencies for a asymmetrical $[0^\circ / 90^\circ / 0^\circ / 90^\circ]$ angle-ply free-free composite beam | 73 |

Chapter 1

Introduction

In the present days, there are different types of composite fiber-reinforced materials available which have been widely used because their strength to weight ratio is very high with respect to the isotropic materials, which is very beneficial from the structural point of view. These laminated composite structures were manufactured by bonding multiple laminated layers together with each other. Since composite materials have anisotropic properties and it shows the coupling behaviour between the different deformation modes, the dynamic characteristics of laminated composite structure can be enhanced by varying the ply orientation and arranging the stacking sequence. Also, in this study, the shear deformation of composite beams has also been considered due to the very high transverse shear to extensional shear modulus ratio.

Here in this study, we consider the dynamics of axially loaded axial-flexural-shear coupled composite beams, based on the Timoshenko beam theory or FSDT theory (first-order shear deformation) for composite beams by proposing a spectral element model. This SEM model is then formulated with the help of variational approach which is then compared for its high accuracy with the other models available in the literature.

In addition to the analytical and exact methods The dynamic analysis of structures

can be carried out mainly by the following methods.

1. Finite Element Method (FEM)
2. Dynamic Stiffness Method (DSM)
3. Spectral Element Method (SEM)
4. Spectral Analysis Method (SAM)

1.1 Finite Element Method

The FEM is itself one of the powerful computational methods, but with the change in the vibration frequency the vibration pattern of a structure varies and also at higher frequencies its wavelength is very small. Hence, the accurate dynamic response will be obtained by capturing all the fundamental high frequencies wave modes. However, the finite element model cannot capture all the wave modes because it is formulated using frequency independent polynomial shape functions. Thus in the higher frequencies where the associated wavelengths are very short, the finite element solution is significantly inaccurate. Now for improving the accuracy of FEM the so-called h-method is used for refining the meshes of FEM model. Unfortunately, from the view of computational aspect, it is not suitable because by refining the meshes of FEM model the size of the required system memory becomes too large and inconvenient.

1.2 Dynamic Stiffness Method

As FEM is deficient in accuracy for higher modes, the alternative approach to increase the accuracy is to use the dynamic shape functions which vary with frequencies and it is frequency dependent. By using DSF, exceptionally high

accuracy can be obtained as it captures all the high frequencies wave modes. This concept is called dynamic stiffness Method (DSM) [1] [2].

In DSM, the accurate dynamic stiffness matrix is utilized which can be planned as a part of the frequency domain. This accurate element shape function can be obtained by utilizing wave arrangement as a part of the frequency domain from the time domain administering differential mathematical statements or governing differential equations. By assuming the harmonic solution of a single frequency, this time domain governing differential equations are transformed into the frequency domain governing differential equations.

1.3 Spectral Analysis Method

Some methods are basically frequency domain methods which are further depend upon time. The Spectral Analysis Method is one of that kind of methods which depends upon time as a function. In this method the solution of governing equation is obtained by superimposing the immense number of wave modes of various frequencies. Fast Fourier transformation is used for solution of this method, which involves frequency domain Fourier coefficient or the persistent Fourier transformation for governing an infinite number of spectral elements then executing the inverse Fourier transformation for obtaining the time history analysis of this solution. Thus when function is very simple in mathematical form or if it is possible to obtain the inverse of that function then it is very feasible to use continuous Fourier transformation for that function. Though it is very tough to operate Fast Fourier Transformation (FFT) for the complex mathematical expression, the Discrete Fourier Transformation (DFT) is widely used in most practical cases.

1.4 Spectral Element Method

By combining all the features of Finite Element Method (FEM) with dynamic stiffness method (DSM) and spectral analysis method (SAM) for the first time Narayanan and Beskos [3] developed a basic concept of spectral element method (SEM) in the year of 1978. Various essential features of this method are as follows:

- **FEM key features:** Assembly of finite elements with spatial discretization or meshing.
- **DSM key features:** With a minimum number of finite element the exact dynamic stiffness matrix can be formulated.
- **SAM key features:** With the help of FFT algorithm and DFT theory, overlapping of different numbers of wave modes is possible.

Advantages of SEM:

- Extremely high accuracy
- Smallness of problem size and degree of freedoms (DOFs)
- Less computational cost
- Very efficient in dealing with frequencies problem
- The system transfer functions
- Very useful in dealing with digitized data
- Locking-free method
- Effective to deal with semi-infinite-domain problems

1.5 Objectives

The prime objectives in this study are presented as follows:

1. To develop laminated composite beam element considering the effect of axial-bending-shear coupled deformation.
2. To develop dynamic stiffness matrix for laminated composite beam element with the help of Spectral Element Method (SEM).
3. To obtain the natural frequencies of composite beams of rectangular cross sections with various boundary conditions.

Chapter 2

Literature Review

There are only a few literature available for the axial-flexural-shear coupled vibration analysis. Some of them consider the axial flexural coupled vibrations in the form of Bernoulli Euler beam theory. Gopalakrishnan and Mahapatra [4] and Sierakowski and Vinson [5] have studied the effect of coupled vibration by using Bernoulli Euler beam theory.

The effect of rotary inertia and shear deformation based on FSDT are first studied by Yang and Chen [6], Abramovich [7], Chandrashekhar et al. [8], Dong et al. [9], Palacz et al. [10], for the flexural-shear coupled vibration analysis of the laminated composite beam. Yang and Chen [6] have used the finite element method for composite laminates and performed the free vibration analysis. Then for different boundary conditions Abramovich [7] and Chandrashekhar et al. [8] studied the exact solutions of natural frequencies for symmetric composite beams. Analysis of wave propagation by Spectral Element model in composite beam has been carried out by Palacz et al. [10]. For finding the mode shapes and natural frequencies of a stepped composite beam, flexural-shear coupled Timoshenko beam model was used by Dong et al. [9].

Teoh and Huang [11] presented an analytical method for free vibration analysis of reinforced composite beam that considers the account of fiber orientation,

rotary inertia and shear deformation. Krishnaswamy et al. [12] used the Lagrange approach to get the solution of the layered composite beam. He used Lagrange approach due to ease in picking displacement functions as these are not dependent upon the various boundary conditions. Abramovich and Livshits [13] used the FSDT theory for free vibration analysis of non-symmetrical composite beam by considering the effect of longitudinal deformation along with shear deformation and rotary inertia. For getting exact natural frequencies Eisenberger et al. [14] used the exact shape function with exact dynamic stiffness matrix. Hassan et al. [15] presented that the change in the fiber orientation would enable the designer to make the structure more stiffened. He also observed that the natural frequencies remain unchanged by changing the material and geometrical properties.

Teboub and Hajela [16] have considered the effect of beam geometry, Poissons ratio, boundary conditions and material anisotropy for analysing the free vibration of symmetrical and non-symmetrical composite beam. By using symbolic computation Maple software, more accurate governing equations are derived leading to calculate more accurate results. Banerjee and Williams [17] studied the coupling between bending and torsional deformation and formulated a dynamic stiffness matrix (DSM) for Timoshenko beam. Lam and Sathiyamoorthy [18] used the Runge-Kutta-Nystrom method for deriving the non-dimensional frequencies of the symmetrical composite beam, non-symmetrical beam, angle-ply laminate and cross-ply laminate. By using Wittrick-Williams algorithm Banerjee [19] analysed a composite Timoshenko beam by considering the effect of shear rigidity, axial force and rotation then he derived the modal frequencies by developing an exact stiffness matrix. Shear Deformation Theory (SDT) was used by Shi and Lam [20] to get stiffness and mass matrices for the laminated composite beam. The high order coupled axial displacement mass matrix showed their exact effect on modal frequencies at higher modes in flexure bending. Bassiouni et al. [21] considered the effect of fiber orientation and shear deformation in finite element model for

finding the natural frequencies. They found that by changing the fiber orientation at core of the beam the modal frequency remain unchanged, and this frequency value increases by increasing the orientation of the outermost fiber of the beam. Bassiouni et al. [21] develop a new method called state space quadrature (SSQD) technique by using elastic theory to analyse free vibration of the laminated beam such as symmetrical and unsymmetrical single-ply, angle-ply, multi-ply, cross-ply.

The in-plane axial displacement is not considered in First order shear deformation theory or Timoshenko beam theory for composite beams. Mahapatra and Gopalakrishnan [22], Chakraborty et al. [23], Ruotolo [24] considered the axial-flexural-shear coupled vibration, and introduced the influence of axial displacement. They used FSDT theory for finding out the different mode shapes and natural frequencies. The FEM model for free vibration and wave propagation of asymmetric composite beam are presented by Chakraborty et al. [23].

Ruotolo [24] and Mahapatra and Gopalakrishnan [22] used force-displacement method for developing the SEM model for symmetric and asymmetric composite beam. In the previous study of SEM modelling Chakraborty et al. [23] and Ruotolo [24] have not considered the effect of axial force and damping coefficient for the composite Timoshenko beam model.

There are many solution methods which are used for composite beams. They are mainly finite element method [6] [23], spectral element method [4] [10] [22] [24] and analytical approaches [7] [8] [9]. In this study the spectral element method is based on the FFT (fast Fourier transforms) which is further depends on DSM (dynamic stiffness method). For satisfying the governing equation, frequency-dependent dynamic shape functions are used to formulate the exact dynamic stiffness matrix and this exactly represents the dynamic behaviour of a structural element. Thus, the spectral element method is often referred as an exact solution method in literatures [25] [26]. Accordingly, in view of the conventional finite element method (FEM), the SEM represents the entire element

of the structure as a single unit, despite of its dimensions, and there is no need for splitting the whole structure into numbers of elements to increase the exactness of the solution. Thus it reduces the total number of degrees of freedoms (DOFs) and the total computational cost as well.

Due to the higher accuracy of Spectral Element Method, this study represents a spectral element model for the analysis of axially loaded axial-flexural-shear coupled composite Timoshenko beams. With the help of variational approach, the spectral element model is formulated and the natural frequencies for different boundary conditions are obtained and the results are compared with the published ones wherever possible.

Chapter 3

Spectral Element model for Composite Timoshenko Beam

3.1 Spectral Element Methodology

The general procedure for analysis of spectral element method is similar to that commonly used for conventional finite element method. And it consists of the following major steps:

- Formulation of governing equation of motion in time domain by Hamiltons Principle.
- Discrete Fourier Transformation (DFT).
- Formulation of governing equation in frequency domain.
- Formulation of Spectral Nodal Forces, Moments and DOFs.
- Formulation of Dynamic shape function.
- Formulation of Spectral Element Equation.
- Weak form of Governing equation.

- Spectral Modal Analysis.
- Formulation of Spectral Matrix.

3.2 Theory of Composite Mechanics

3.2.1 Three-Dimensional Stress Strain Relationship

The stress-strain relationships for orthotropic materials in the coordinates aligned with its principal material coordinates (1,2,3) are given by,

$$\begin{Bmatrix} \sigma_1 \\ \sigma_2 \\ \sigma_3 \\ \sigma_4 \\ \sigma_5 \\ \sigma_6 \end{Bmatrix} = \begin{bmatrix} C_{11} & C_{12} & C_{13} & 0 & 0 & 0 \\ C_{12} & C_{22} & C_{23} & 0 & 0 & 0 \\ C_{13} & C_{23} & C_{33} & 0 & 0 & 0 \\ 0 & 0 & 0 & C_{44} & 0 & 0 \\ 0 & 0 & 0 & 0 & C_{55} & 0 \\ 0 & 0 & 0 & 0 & 0 & C_{66} \end{bmatrix} \begin{Bmatrix} \varepsilon_1 \\ \varepsilon_2 \\ \varepsilon_3 \\ \varepsilon_4 \\ \varepsilon_5 \\ \varepsilon_6 \end{Bmatrix} \quad (3.1)$$

where $\varepsilon_j (j = 1, 2, \dots, 6)$ are the strain components, and $\sigma_j (j = 1, 2, \dots, 6)$ are the stress components, $c_{ij} (i, j = 1, 2, \dots, 6)$ are the stiffness coefficients or the compliance coefficients. Then the stress strain relationship can be written as,

$$\begin{Bmatrix} \varepsilon_1 \\ \varepsilon_2 \\ \varepsilon_3 \\ \varepsilon_4 \\ \varepsilon_5 \\ \varepsilon_6 \end{Bmatrix} = \begin{bmatrix} S_{11} & S_{12} & S_{13} & 0 & 0 & 0 \\ S_{12} & S_{22} & S_{23} & 0 & 0 & 0 \\ S_{13} & S_{23} & S_{33} & 0 & 0 & 0 \\ 0 & 0 & 0 & S_{44} & 0 & 0 \\ 0 & 0 & 0 & 0 & S_{55} & 0 \\ 0 & 0 & 0 & 0 & 0 & S_{66} \end{bmatrix} \begin{Bmatrix} \sigma_1 \\ \sigma_2 \\ \sigma_3 \\ \sigma_4 \\ \sigma_5 \\ \sigma_6 \end{Bmatrix} \quad (3.2)$$

The c_{ij} are the stiffness coefficients which are determined from nine independent

engineering constants as follows:

$$\begin{aligned} S_{11} &= \frac{1}{E_1}, & S_{22} &= \frac{1}{E_2}, & S_{33} &= \frac{1}{E_3} \\ S_{44} &= \frac{1}{G_{23}}, & S_{55} &= \frac{1}{G_{31}}, & S_{66} &= \frac{1}{G_{12}} \\ S_{12} &= -\frac{\nu_{21}}{E_2}, & S_{13} &= -\frac{\nu_{31}}{E_3}, & S_{23} &= -\frac{\nu_{32}}{E_3} \end{aligned} \quad (3.3)$$

Here the subscripts denotes the local coordinates axis (1,2,3) and following are the stress and strains component used:

$$\begin{aligned} \sigma_1 &= \sigma_{11}, \quad \sigma_2 = \sigma_{22}, \quad \sigma_3 = \sigma_{33}, \quad \sigma_4 = \sigma_{23}, \quad \sigma_5 = \sigma_{31}, \quad \sigma_6 = \sigma_{12} \\ \varepsilon_1 &= \varepsilon_{11}, \quad \varepsilon_2 = \varepsilon_{22}, \quad \varepsilon_3 = \varepsilon_{33}, \quad \varepsilon_4 = 2\varepsilon_{23}, \quad \varepsilon_5 = 2\varepsilon_{31}, \quad \varepsilon_6 = 2\varepsilon_{12} \end{aligned} \quad (3.4)$$

3.2.2 Stress-Strain Relationships for an Orthotropic Lamina

We know that for an orthotropic lamina, $\sigma_3 = 0$. Thus, from Eq.(3.2) we have,

$$\varepsilon_3 = S_{13}\sigma_1 + S_{23}\sigma_2 \quad (3.5)$$

and the Eq.(3.2) can be rewritten as,

$$\begin{Bmatrix} \varepsilon_1 \\ \varepsilon_2 \\ \varepsilon_6 \end{Bmatrix} = \begin{bmatrix} S_{11} & S_{12} & 0 \\ S_{12} & S_{22} & 0 \\ 0 & 0 & S_{66} \end{bmatrix} \begin{Bmatrix} \sigma_1 \\ \sigma_2 \\ \sigma_6 \end{Bmatrix} \quad (3.6)$$

and

$$\begin{Bmatrix} \varepsilon_4 \\ \varepsilon_5 \end{Bmatrix} = \begin{bmatrix} S_{44} & 0 \\ 0 & S_{55} \end{bmatrix} \begin{Bmatrix} \sigma_4 \\ \sigma_5 \end{Bmatrix} \quad (3.7)$$

From Eq.(3.6) and Eq.(3.7) we obtain the stress strain relationships for an orthotropic lamina as,

$$\begin{Bmatrix} \sigma_1 \\ \sigma_2 \\ \sigma_6 \end{Bmatrix} = \begin{bmatrix} Q_{11} & Q_{12} & 0 \\ Q_{12} & Q_{22} & 0 \\ 0 & 0 & Q_{66} \end{bmatrix} \begin{Bmatrix} \varepsilon_1 \\ \varepsilon_2 \\ \varepsilon_6 \end{Bmatrix} \quad (3.8)$$

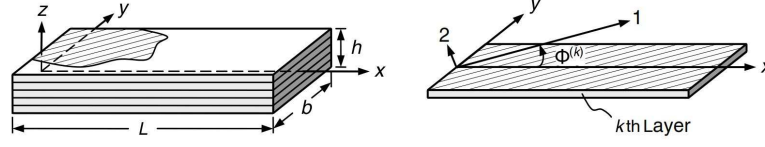


Figure 3.1: The global and local coordinate systems for a composite laminated beam

and

$$\begin{Bmatrix} \sigma_4 \\ \sigma_5 \end{Bmatrix} = \begin{bmatrix} Q_{44} & 0 \\ 0 & Q_{55} \end{bmatrix} \begin{Bmatrix} \varepsilon_4 \\ \varepsilon_5 \end{Bmatrix} \quad (3.9)$$

Here Q_{mn} are the reduced stiffnesses given by

$$\begin{aligned} Q_{11} &= \frac{S_{22}}{S_{11}S_{22} - S_{12}^2} = \frac{E_1}{1 - \nu_{12}\nu_{21}} \\ Q_{22} &= \frac{S_{11}}{S_{11}S_{22} - S_{12}^2} = \frac{E_2}{1 - \nu_{12}\nu_{21}} \\ Q_{12} &= \frac{-S_{12}}{S_{11}S_{22} - S_{12}^2} = \frac{\nu_{21}E_1}{1 - \nu_{12}\nu_{21}} = \frac{\nu_{12}E_2}{1 - \nu_{12}\nu_{21}} \\ Q_{44} &= \frac{1}{S_{44}} = G_{23}, \\ Q_{55} &= \frac{1}{S_{55}} = G_{31}, \\ Q_{66} &= \frac{1}{S_{66}} = G_{12}, \end{aligned} \quad (3.10)$$

Now the stress relationship from Fig(3.1) for global coordinates (x, y, z) and local coordinates $(1, 2, 3)$ are obtained by rotating the xy -plane counter clockwise about the z -axis by an angle ϕ then the coordinate transformation matrices are given by:

$$\begin{Bmatrix} \sigma_{xx} \\ \sigma_{yy} \\ \sigma_{xy} \end{Bmatrix} = \begin{bmatrix} \cos^2\phi & \sin^2\phi & -\sin 2\phi \\ \sin^2\phi & \cos^2\phi & \sin 2\phi \\ \sin\phi\cos\phi & -\sin\phi\cos\phi & \cos^2\phi - \sin^2\phi \end{bmatrix} \begin{Bmatrix} \sigma_1 \\ \sigma_2 \\ \sigma_6 \end{Bmatrix} \quad (3.11)$$

and

$$\begin{Bmatrix} \sigma_{yz} \\ \sigma_{zx} \end{Bmatrix} = \begin{bmatrix} \cos\phi & \sin\phi \\ -\sin\phi & \cos\phi \end{bmatrix} \begin{Bmatrix} \sigma_4 \\ \sigma_5 \end{Bmatrix}$$

The strain relationship between the axes are

$$\begin{Bmatrix} \varepsilon_{xx} \\ \varepsilon_{yy} \\ \gamma_{xy} \end{Bmatrix} = \begin{bmatrix} \cos^2\phi & \sin^2\phi & -\sin 2\phi \\ \sin^2\phi & \cos^2\phi & \sin 2\phi \\ \sin\phi\cos\phi & -\sin\phi\cos\phi & \cos^2\phi - \sin^2\phi \end{bmatrix} \begin{Bmatrix} \varepsilon_1 \\ \varepsilon_2 \\ \varepsilon_6 \end{Bmatrix} \quad (3.12)$$

and

$$\begin{Bmatrix} \gamma_{yz} \\ \gamma_{zx} \end{Bmatrix} = \begin{bmatrix} \cos\phi & \sin\phi \\ -\sin\phi & \cos\phi \end{bmatrix} \begin{Bmatrix} \varepsilon_4 \\ \varepsilon_5 \end{Bmatrix}$$

where

$$\gamma_{xy} = 2\varepsilon_{xy}, \quad \gamma_{yz} = 2\varepsilon_{yz}, \quad \gamma_{zx} = 2\varepsilon_{zx} \quad (3.13)$$

Now from Eq.(3.8) and Eq.(3.9) the stress-strain relationships with respect to the global coordinates (x,y,z) is given by,

$$\begin{Bmatrix} \sigma_{xx} \\ \sigma_{yy} \\ \sigma_{xy} \end{Bmatrix} = \begin{bmatrix} \bar{Q}_{11} & \bar{Q}_{12} & \bar{Q}_{16} \\ \bar{Q}_{12} & \bar{Q}_{22} & \bar{Q}_{26} \\ \bar{Q}_{16} & \bar{Q}_{26} & \bar{Q}_{66} \end{bmatrix} \begin{Bmatrix} \varepsilon_{xx} \\ \varepsilon_{yy} \\ \varepsilon_{xy} \end{Bmatrix} \quad (3.14)$$

and

$$\begin{Bmatrix} \sigma_{yz} \\ \sigma_{zx} \end{Bmatrix} = \begin{bmatrix} \bar{Q}_{44} & \bar{Q}_{45} \\ \bar{Q}_{45} & \bar{Q}_{55} \end{bmatrix} \begin{Bmatrix} \gamma_{yz} \\ \gamma_{zx} \end{Bmatrix} \quad (3.15)$$

The transformed reduced stiffnesses \bar{Q}^{ij} are given by:

$$\begin{aligned}
\bar{Q}_{11} &= Q_{11}\cos^4\phi + Q_{22}\sin^4\phi + 2(Q_{12} + 2Q_{66})\sin^2\phi\cos^2\phi \\
\bar{Q}_{22} &= Q_{11}\sin^4\phi + Q_{22}\cos^4\phi + 2(Q_{12} + 2Q_{66})\sin^2\phi\cos^2\phi \\
\bar{Q}_{66} &= Q_{66}(\sin^4\phi + \cos^4\phi) + (Q_{11} + Q_{22} - 2Q_{12} - 2Q_{66})\sin^2\phi\cos^2\phi \\
\bar{Q}_{12} &= Q_{12}(\sin^4\phi + \cos^4\phi) + (Q_{11} + Q_{22} - 4Q_{66})\sin^2\phi\cos^2\phi \\
\bar{Q}_{16} &= (Q_{11} - Q_{12} - 2Q_{66})\sin\phi\cos^3\phi + (Q_{12} - Q_{22} + 2Q_{66})\sin^3\phi\cos\phi \\
\bar{Q}_{26} &= (Q_{11} - Q_{12} - 2Q_{66})\sin^3\phi\cos\phi + (Q_{12} - Q_{22} + 2Q_{66})\sin\phi\cos^3\phi \\
\bar{Q}_{44} &= Q_{44}\cos^2\phi + Q_{55}\sin^2\phi \\
\bar{Q}_{55} &= Q_{55}\cos^2\phi + Q_{44}\sin^2\phi \\
\bar{Q}_{45} &= (Q_{55} - Q_{44})\cos\phi\sin\phi
\end{aligned} \tag{3.16}$$

3.2.3 Strain-Displacement Relationships

The strains are given by,

$$\begin{aligned}
\varepsilon_{xx} &= \frac{\partial u}{\partial x}, \quad \varepsilon_{yy} = \frac{\partial v}{\partial y}, \quad \gamma_{xy} = 2\varepsilon_{xy} = \frac{\partial v}{\partial x} + \frac{\partial u}{\partial y} \\
\gamma_{yz} &= 2\varepsilon_{yz} = \frac{\partial w}{\partial y} + \frac{\partial v}{\partial z}, \quad \gamma_{zx} = 2\varepsilon_{zx} = \frac{\partial w}{\partial x} + \frac{\partial u}{\partial z}
\end{aligned} \tag{3.17}$$

$u(x, y, z, t)$, $v(x, y, z, t)$, and $w(x, y, z, t)$ represent the displacements in the x,y and z direction, respectively.whose general form is given as

$$\begin{aligned}
u(x, y, z, t) &= u_0(x, y, t) - z\theta_x(x, y, t) \\
v(x, y, z, t) &= -z\theta_y(x, y, t) \\
w(x, y, z, t) &= w_0(x, y, t)
\end{aligned} \tag{3.18}$$

where w_0 and u_0 are the displacements of a point where subscript 0 denotes the reference plane $z = 0$ in the x and z direction, and θ_x and θ_y are the slope along

x -axis and y -axis respectively. By solving Eq.(3.18) and Eq.(3.17), we have

$$\begin{aligned}\gamma_{yz} &= \frac{\partial w_0}{\partial y} - \theta_y, & \gamma_{zx} &= \frac{\partial w_0}{\partial x} - \theta_x \\ \varepsilon_{xx} &= \varepsilon_{yy} = z\chi_y, & \gamma_{xy} &= \gamma_{xy}^0 + z\chi_{xy}\end{aligned}\quad (3.19)$$

the in-plane strains ε_{xx}^0 , ε_{yy}^0 and ε_{xy}^0 are given by

$$\varepsilon_{xx}^0 = \frac{\partial u_0}{\partial x}, \quad \gamma_{xy}^0 = \frac{\partial u_0}{\partial y} \quad (3.20)$$

the curvatures χ_x , χ_y and χ_{xy} are given by,

$$\begin{aligned}\chi_x &= -\frac{\partial \theta_x}{\partial x}, & \chi_y &= -\frac{\partial \theta_y}{\partial y} \\ \chi_{xy} &= -\left(\frac{\partial \theta_y}{\partial x} + \frac{\partial \theta_x}{\partial y}\right)\end{aligned}\quad (3.21)$$

3.2.4 Resultant Forces and Moments

The Resultant moments and forces are obtained by integrating the stresses throughout the thickness of laminate ($-h/2$ to $h/2$) as

$$\begin{Bmatrix} N_x \\ Q_x \end{Bmatrix} = \int_{-\frac{h}{2}}^{\frac{h}{2}} \begin{Bmatrix} \sigma_{xx} \\ \kappa \sigma_{zx} \end{Bmatrix} dz = \sum_{k=1}^N \int_{z_{k-1}}^{z_k} \begin{Bmatrix} \sigma_{xx}^{(k)} \\ \kappa \sigma_{zx}^{(k)} \end{Bmatrix} dz \quad (3.22)$$

$$\begin{Bmatrix} M_{xx} \\ M_{yy} \\ M_{xy} \end{Bmatrix} = \int_{-\frac{h}{2}}^{\frac{h}{2}} \begin{Bmatrix} \sigma_{xx} \\ \sigma_{yy} \\ \sigma_{xy} \end{Bmatrix} z dz = \sum_{k=1}^N \int_{z_{k-1}}^{z_k} \begin{Bmatrix} \sigma_{xx}^{(k)} \\ \sigma_{yy}^{(k)} \\ \sigma_{xy}^{(k)} \end{Bmatrix} z dz \quad (3.23)$$

where h is the total thickness of the laminated composite beam, b is the total width of the beam, κ is shear correction factor and z_k and z_{k-1} are defined by Fig.(3.2).

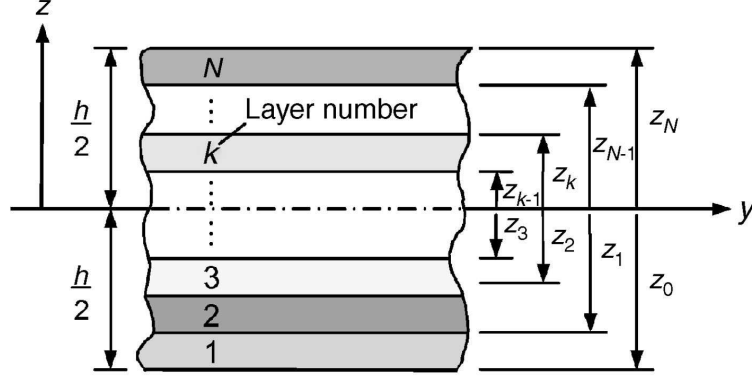


Figure 3.2: Geometry of an N-layered laminate

Also for the k^{th} layer the stress-strain relationship are taken from Eq.(3.14) and Eq.(3.15) as,

$$\begin{Bmatrix} \sigma_{xx}^{(k)} \\ \sigma_{yy}^{(k)} \\ \sigma_{xy}^{(k)} \end{Bmatrix} = \begin{bmatrix} \bar{Q}_{11}^{(k)} & \bar{Q}_{12}^{(k)} & \bar{Q}_{16}^{(k)} \\ \bar{Q}_{12}^{(k)} & \bar{Q}_{22}^{(k)} & \bar{Q}_{26}^{(k)} \\ \bar{Q}_{16}^{(k)} & \bar{Q}_{26}^{(k)} & \bar{Q}_{66}^{(k)} \end{bmatrix} \begin{Bmatrix} \varepsilon_{xx}^{(k)} \\ \varepsilon_{yy}^{(k)} \\ \gamma_{xy}^{(k)} \end{Bmatrix} \quad (3.24)$$

Now,

$$\sigma_{zx}^{(k)} = \begin{bmatrix} \bar{Q}_{45}^{(k)} & \bar{Q}_{55}^{(k)} \end{bmatrix} \begin{Bmatrix} \gamma_{zy}^{(k)} \\ \gamma_{zx}^{(k)} \end{Bmatrix} \quad (3.25)$$

Now by putting Eq.(3.19) into Eq.(3.24) and Eq.(3.25) and solving this equation and substituting the result into Eq.(3.22) and Eq.(3.23), we have the expression as

$$N_x = A_{11}\varepsilon_{xx}^0 + A_{16}\gamma_{xy}^0 + B_{11}\chi_x + B_{12}\chi_y + B_{16}\chi_{xy} \quad (3.26)$$

$$Q_x = \kappa A_{45} \left(\frac{\partial w_0}{\partial y} - \theta_y \right) + \kappa A_{55} \left(\frac{\partial w_0}{\partial x} - \theta_x \right) \quad (3.27)$$

$$\begin{Bmatrix} M_{xx} \\ M_{yy} \\ M_{xy} \end{Bmatrix} = \begin{bmatrix} B_{11} & B_{16} \\ B_{12} & B_{26} \\ B_{16} & B_{66} \end{bmatrix} \begin{Bmatrix} \varepsilon_{xx}^0 \\ \gamma_{xy}^0 \end{Bmatrix} + \begin{bmatrix} D_{11} & D_{12} & D_{16} \\ D_{12} & D_{22} & D_{26} \\ D_{16} & D_{26} & D_{66} \end{bmatrix} \begin{Bmatrix} \chi_x \\ \chi_y \\ \chi_{xy} \end{Bmatrix} \quad (3.28)$$

where

$$\begin{aligned}
 A_{ij} &= \sum_{k=1}^N \bar{Q}_{ij}^{(k)} (z_k - z_{k-1}) \\
 B_{ij} &= \frac{1}{2} \sum_{k=1}^N \bar{Q}_{ij}^{(k)} (z_k^2 - z_{k-1}^2) \\
 D_{ij} &= \frac{1}{3} \sum_{k=1}^N \bar{Q}_{ij}^{(k)} (z_k^3 - z_{k-1}^3)
 \end{aligned} \tag{3.29}$$

3.3 Equations of Motion for Symmetrical Composite Laminated Beams

For Simply supported T-beam, the free vibration of a uniform Timoshenko beam is given by,

$$\begin{aligned}
 \kappa GA (w'' - \theta') - \rho A \ddot{w} &= 0 \\
 EI \theta'' + \kappa GA (w' - \theta) - \rho I \ddot{\theta} &= 0
 \end{aligned} \tag{3.30}$$

where,

$w(x, t)$ = Transverse displacement

$\theta(x, t)$ = Slope due to bending respectively

E = Young's modulus

G = Shear modulus

κ = Shear correction factor (depend upon the shape of the cross section)

A = Cross-sectional area

I = Area moment of inertia about neutral axis

The internal bending moment and transverse shear force are given by,

$$\begin{aligned} Q_t(x, t) &= \kappa GA [w'(x, t) - \theta(x, t)] \\ M_t(x, t) &= EI\theta'(x, t) \end{aligned} \quad (3.31)$$

Assuming the solution of Equation (3.30) in the spectral form as

$$\begin{aligned} w(x, t) &= \frac{1}{N} \sum_{n=0}^{N-1} W_n(x; \omega_n) e^{i\omega_n t} \\ \theta(x, t) &= \frac{1}{N} \sum_{n=0}^{N-1} \Theta_n(x; \omega_n) e^{i\omega_n t} \end{aligned} \quad (3.32)$$

Substituting the Eq (3.32) into Eq (3.30) gives the eigenvalue problem as

$$\begin{aligned} \kappa GA (W'' - \Theta') - \rho A \omega^2 W &= 0 \\ EI\Theta'' + \kappa GA (W' - \Theta) + \Theta \rho I \omega^2 &= 0 \end{aligned} \quad (3.33)$$

Assuming the general solution to Eq. (3.33) as

$$\begin{aligned} W(x) &= a e^{-ik(\omega)x} \\ \Theta(x) &= \alpha a e^{-ik(\omega)x} \end{aligned} \quad (3.34)$$

Now substituting the Eq. (3.34) into Eq. (3.33) to obtain the eigenvalue problem as,

$$\begin{bmatrix} \kappa GA k^2 - \rho A \omega^2 & -ik\kappa GA \\ ik\kappa GA & EI k^2 + \kappa GA - \rho I \omega^2 \end{bmatrix} \begin{Bmatrix} 1 \\ \alpha \end{Bmatrix} = \begin{Bmatrix} 0 \\ 0 \end{Bmatrix} \quad (3.35)$$

Eq. (3.35) gives a dispersion relation as

$$k^4 - \xi k_F^4 k^2 - k_F^4 (1 - \xi_1 k_G^4) = 0 \quad (3.36)$$

where

$$k_F = \sqrt{\omega} \left(\frac{\rho A}{EI} \right)^{\frac{1}{4}}, \quad k_G = \sqrt{\omega} \left(\frac{\rho A}{\kappa GA} \right)^{\frac{1}{4}} \quad (3.37)$$

and

$$\xi = \xi_1 + \xi_2, \quad \xi_1 = \frac{\rho I}{\rho A}, \quad \xi_2 = \frac{EI}{\kappa GA} \quad (3.38)$$

By solving Eq. (3.36) we obtain four roots as

$$k_1 = -k_2 = \frac{1}{\sqrt{2}} k_F \sqrt{\xi k_F^2 + \sqrt{\xi^2 k_F^4 + 4(1 - \xi_1 k_G^4)}} = k_t \quad (3.39)$$

$$k_3 = -k_4 = \frac{1}{\sqrt{2}} k_F \sqrt{\xi k_F^2 - \sqrt{\xi^2 k_F^4 + 4(1 - \xi_1 k_G^4)}} = k_e$$

From the first line of Eq. (3.35), we can obtain the wavemode ratio as

$$\alpha_p(\omega) = \frac{1}{ik_p} (k_p^2 - k_G^4) = -ir_p(\omega) \quad (p = 1, 2, 3, 4) \quad (3.40)$$

where

$$r_p(\omega) = \frac{1}{k_p} (k_p^2 - k_G^4) \quad (3.41)$$

it is noted that when $\xi = 0$ and $k_G = 0$, Eq.(3.36) is reduced to the dispersion equation for the Bernoulli-Euler beam and from Eq.(3.39) the wave-numbers become identical with those of Bernoulli-Euler beam.

By using this four wavenumbers which is given by Eq.(3.39), the general solution of Eq.(3.33) can be written as

$$\begin{aligned} W(x) &= a_1 e^{-ik_t x} + a_2 e^{+ik_t x} + a_3 e^{-ik_e x} + a_4 e^{+ik_e x} = \mathbf{e}_w(\mathbf{x}; \omega) \mathbf{a} \\ \Theta(x) &= \alpha_1 a_1 e^{-ik_t x} + \alpha_2 a_2 e^{+ik_t x} + \alpha_3 a_3 e^{-ik_e x} + \alpha_4 a_4 e^{+ik_e x} = \mathbf{e}_\theta(\mathbf{x}; \omega) \mathbf{a} \end{aligned} \quad (3.42)$$

where

$$\mathbf{a} = \{a_1 \ a_2 \ a_3 \ a_4\}^T \quad (3.43)$$

$$e_w(x; \omega) = [e^{-ik_t x} \ e^{+ik_t x} \ e^{-ik_e x} \ e^{+ik_e x}] \quad (3.44)$$

$$e_\theta(x; \omega) = e_w(x; \omega) \mathbf{B}(\omega)$$

$$\mathbf{B}(\omega) = \text{diag}[\alpha_p(\omega)]$$

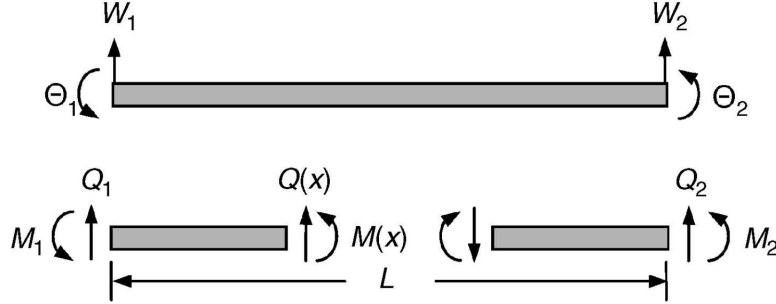


Figure 3.3: Sign convention for the Timoshenko-beam element

The relation between the slope and spectral nodal displacements of the finite T-beam element of length L Fig. (3.3) and its relative displacement fields are give by,

$$\mathbf{d} = \begin{Bmatrix} W_1 \\ \Theta_1 \\ W_2 \\ \Theta_2 \end{Bmatrix} = \begin{Bmatrix} W(0) \\ \Theta(0) \\ W(L) \\ \Theta(L) \end{Bmatrix} \quad (3.45)$$

Substituting Eq.(3.42) into the right-hand side of Eq.(3.45) gives

$$\mathbf{d} = \begin{bmatrix} e_w(0; \omega) \\ e_\theta(0; \omega) \\ e_w(L; \omega) \\ e_\theta(L; \omega) \end{bmatrix} \mathbf{a} = \mathbf{H}_T(\omega) \mathbf{a} \quad (3.46)$$

where

$$\mathbf{H}_T(\omega) = \begin{bmatrix} 1 & 1 & 1 & 1 \\ -ir_t & ir_t & -ir_e & ir_e \\ e_t & e_t^{-1} & e_e & e_e^{-1} \\ -ir_t e_t & ir_t e_t^{-1} & -ir_e e_e & ir_e e_e^{-1} \end{bmatrix} \quad (3.47)$$

with the use of following definitions:

$$\begin{aligned} e_t &= e^{-ik_t L}, & e_e &= e^{-ik_e L} \\ r_t &= \frac{1}{k_t}(k_t^2 - k_G^4), & r_e &= \frac{1}{k_e}(k_e^2 - k_G^4) \end{aligned} \quad (3.48)$$

With the help of Eq.(3.46), the constant vector \mathbf{a} can be eliminated from the Eq.(3.42) and the general solutions can be written as,

$$W(x) = N_w(x; \omega)d, \quad \Theta(x) = N_\theta(x; \omega)d \quad (3.49)$$

where,

$$\begin{aligned} N_w(x; \omega) &= e_w(x; \omega)\mathbf{H}_T^{-1}(\omega) \\ N_\theta(x; \omega) &= e_\theta(x; \omega)\mathbf{H}_T^{-1}(\omega) = e_w(x; \omega)\mathbf{B}(\omega)\mathbf{H}_T^{-1}(\omega) \end{aligned} \quad (3.50)$$

Now from Eq.(3.31), the spectral component of the transverse shear and bending moment are related to $\Theta(x)$ and $W(x)$ by,

$$Q = \kappa GA(W' - \Theta), \quad M = EI\Theta' \quad (3.51)$$

The relation between the spectral nodal transverse shear force and bending moments from Fig. (3.3) of the finite T-beam element and the corresponding forces and moments are given by,

$$f_c(\omega) = \begin{Bmatrix} Q_1 \\ M_1 \\ Q_2 \\ M_2 \end{Bmatrix} = \begin{Bmatrix} -Q(0) \\ -M(0) \\ +Q(L) \\ +M(L) \end{Bmatrix} \quad (3.52)$$

Substituting Eq.(3.50) to Eq.(3.49) and solving we have,

$$\begin{aligned} W(x) &= e_w(x; \omega) \mathbf{H}_T^{-1} \mathbf{d} \\ \Theta(x) &= e_\theta(x; \omega) \mathbf{H}_T^{-1} \mathbf{d} \end{aligned} \quad (3.53)$$

Substituting Eq.(3.53) and Eq.(3.51) into the right hand side of Eq.(3.52) and solving we have,

$$f_c = \begin{Bmatrix} -EIW'''(0) \\ -EIW''(0) \\ EIW'''(L) \\ EIW''(L) \end{Bmatrix} = \begin{Bmatrix} -\kappa GAe'_w(0; \omega) - e_\theta(0; \omega) \\ -EIe'_\theta(0; \omega) \\ \kappa GAe'_w(L; \omega) - e_\theta(L; \omega) \\ EIe'_\theta(L; \omega) \end{Bmatrix} \mathbf{H}_T^{-1} \mathbf{d} = \mathbf{S}_T(\omega) \mathbf{d} \quad (3.54)$$

where $\mathbf{S}_T(\omega)$ is a spectral element matrix or dynamic stiffness matrix for the beam element, and it is given by,

$$\mathbf{S}_T(\omega) = \begin{Bmatrix} -\kappa GAe'_w(0; \omega) - e_\theta(0; \omega) \\ -EIe'_\theta(0; \omega) \\ \kappa GAe'_w(L; \omega) - e_\theta(L; \omega) \\ EIe'_\theta(L; \omega) \end{Bmatrix} \mathbf{H}_T^{-1} \quad (3.55)$$

Here, f_c is the nodal force vector associated with the concentrated dynamic forces applied at the nodes of the beam.

3.4 Equations of Motion for Non Symmetrical Composite Laminated Beams

Let us assume a uniform composite beam which can take a small magnitude of axial-flexural-shear coupled vibration. The dimensions of the composite beam are of length L , thickness h and the width b , as shown in the figure (3.1). The x-axis is passes through the shear center of the beam which also coincides with the elastic axis. In Fig. (3.1) the system coordinates illustrate the material coordinates for an

individual laminate ply, which is revolved about z-axis (or 3-axis) by a definite ply orientation angle ϕ with respect to the inertial reference coordinates system (x,y,z) . The axial and bending deflection is given by $u_0(x, t)$ and $w_0(x, t)$ respectively. Now by using FSDT theory the mid plane displacements of composite beam is given by,

$$\begin{aligned} w(x, y, z, t) &\cong w_0(x, t) \\ u(x, y, z, t) &\cong u_0(x, t) - z\theta(x, t) \end{aligned} \quad (3.56)$$

where $\theta(x, t)$ is the mid-plane rotation about y and z axis respectively.

Now, following equation describes the relation of bending moment $M(x, t)$ and axial force $N(x, t)$ with rotation $\theta(x, t)$ and displacement $u_0(x, t)$ [8] [24] [30]

$$\begin{Bmatrix} N \\ M \end{Bmatrix} = \begin{bmatrix} EA & -K \\ -K & EI \end{bmatrix} \begin{Bmatrix} u'_0 \\ \theta' \end{Bmatrix} \quad (3.57)$$

where K , EI , and EA are the axial-flexural material coupling rigidity, flexural rigidity and axial rigidity respectively, and they are defined by:

$$EI = bD_{11}, \quad K = bB_{11}, \quad EA = bA_{11} \quad (3.58)$$

Similarly, the following equation describe the relationship between transverse shear force $Q(x, t)$ with rotation $\theta(x, t)$ and axial displacement $u_0(x, t)$ [8] [24] [30]:

$$Q(x, t) = \kappa GA(w'_0 - \theta) \quad (3.59)$$

where κGA is the apparent shear rigidity given by:

$$\kappa GA = b\kappa A_{55} \quad (3.60)$$

where κ is the shear correction factor for composite beam. Now by Eq.(3.58) and (3.60), the equation for A_{11} , B_{11} , D_{11} and A_{55} are,

$$\begin{aligned}
(A_{11}, B_{11}, D_{11}) &= \sum_k \int_{z_{k-1}}^{z_k} \bar{Q}_{11}(1, z, z^2) dz \\
A_{55} &= \sum_k \int_{z_{k-1}}^{z_k} \bar{Q}_{55} dz
\end{aligned} \tag{3.61}$$

where z_k and z_{k-1} are the thickness of the k th layer as shown in Fig.(3.2) and \bar{Q}_{55} and \bar{Q}_{11} are the reduced stiffness's transformed matrix derived from Reddy [29].

The governing differential equations of motion and the associated boundary conditions for composite laminated beam are derived from Hamilton's principle given by:

$$\int_0^t (\delta T - \delta V + \delta W) dt = 0 \tag{3.62}$$

where T is the kinetic energy, V is the strain energy, and δW is the virtual work done by external forces.

The strain energy and kinetic energy are given by:

$$\begin{aligned}
U &= \frac{1}{2} \int_0^L \{ N u_0' - M \chi_x + Q (w_0' - \theta) + P w_0'^2 \} dx \\
&= \frac{1}{2} \int_0^L \{ E A u_0'^2 - 2 K u_0' \theta' + E I \theta'^2 + \kappa G A (w_0' - \theta)^2 + P w_0'^2 \} dx
\end{aligned} \tag{3.63}$$

and

$$\begin{aligned}
T &= \frac{1}{2} \int_0^L \int_{-\frac{h}{2}}^{\frac{h}{2}} \rho b (\dot{w}^2 + \dot{u}^2) dz dx \\
&= \frac{1}{2} \int_0^L (\rho A \dot{w}_0^2 + \rho A \dot{u}_0^2 - 2 \rho R \dot{u}_0 \dot{\theta} + \rho I \dot{\theta}^2) dx
\end{aligned} \tag{3.64}$$

where

$$(\rho A, \rho R, \rho I) = b \int_{-\frac{h}{2}}^{\frac{h}{2}} \rho (1, z, z^2) dz \tag{3.65}$$

where

ρ = mass density

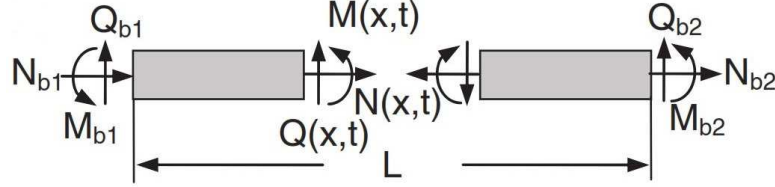


Figure 3.4: Sign convention and boundary forces for composite Timoshenko beam element



Figure 3.5: Spectral nodal DOFs and forces for composite Timoshenko beam element

ρA = apparent mass of the beam

ρR = apparent first order mass moment of inertia

ρI = apparent second order mass moment of inertia

All the above values are considered as per unit length. The different type of external forces applied on the beam are shown in Fig.(3.4) and they are:

$N_{r1}(t)$ and $N_{r2}(t)$ = axial forces

$M_{r1}(t)$ and $M_{r2}(t)$ = bending moments

$Q_{r1}(t)$ and $Q_{r2}(t)$ = transverse forces

Here the subscript 1 refers to a point on the beam at $x = 0$, and the subscript 2 is a point on the beam at $x = L$. All the distributed loads such

as $f_u(x, t)$, $f_w(x, t)$, and $f_\theta(x, t)$, as well as the tensile axial force P which is constant, are acted in x -direction through the mass center of the cross-section of the laminated composite beam. The virtual work done δW by the viscous damping and external forces are given by:

$$\begin{aligned} \delta W = & N_{r1}\delta u_0(0) + N_{r2}\delta u_0(L) + M_{r1}\delta\theta(0) + M_{r2}\delta\theta(L) \\ & + Q_{r1}\delta w_0(0) + Q_{r2}\delta w_0(L) \\ & + \int_0^L [f_u(x, t)\delta u_0 + f_w(x, t)\delta w_0 + f_\theta(x, t)\delta\theta \\ & - c_1\dot{u}_0 - c_2\dot{w}_0\delta w_0 - c_3\dot{\theta}\delta\theta]dx \end{aligned} \quad (3.66)$$

where c_1, c_2 and c_3 are viscous damping coefficients. Now by substituting Eq.(3.64) and Eq.(3.66) into Eq.(3.62) and applying integral by parts into Eq.(3.62) we have,

$$\begin{aligned} \int_0^t [\int_0^L \{ & [EAu_0'' - K\theta'' - \rho A\ddot{u}_0 + \rho R\ddot{\theta} - c_1\dot{u}_0 + f_u(x, t)]\delta u_0 \\ & + [\kappa GA(w_0'' - \theta') + Pw_0'' - \rho A\ddot{w}_0 - c_2\dot{w}_0 + f_w(x, t)]\delta w_0 \\ & + [EI\theta'' + \kappa GA(w_0' - \theta) - Ku_0'' + \rho R\ddot{u}_0 - \rho I\ddot{\theta} - c_3\dot{\theta} \\ & + f_\theta(x, t)]\delta\theta \} dx - N(x, t)\delta u_0|_0^L - M(x, t)\delta\theta|_0^L \\ & - [Q(x, t) + Pw_0']\delta w_0|_0^L + N_{r1}\delta u_0(0) + N_{r2}\delta u_0(L) \\ & + M_{r1}\delta\theta(0) + M_{r2}\delta\theta(L) + Q_{r1}\delta w_0(0) + Q_{r2}\delta w_0(L)] dt = 0 \end{aligned} \quad (3.67)$$

We can obtain from Eq.(3.67) the three governing equations of motion as:

$$\begin{aligned} EAu_0'' - K\theta'' - \rho A\ddot{u}_0 + \rho R\ddot{\theta} - c_1\dot{u}_0 + f_u(x, t) & = 0 \\ \kappa GA(w_0'' - \theta') + Pw_0'' - \rho A\ddot{w}_0 - c_2\dot{w}_0 + f_w(x, t) & = 0 \\ EI\theta'' + \kappa GA(w_0' - \theta) - Ku_0'' + \rho R\ddot{u}_0 - \rho I\ddot{\theta} - c_3\dot{\theta} + f_\theta(x, t) & = 0 \end{aligned} \quad (3.68)$$

and the geometric boundary conditions are:

$$\begin{aligned}
N(0, t) &= -N_{r1}(t) & \text{or} & & u_0(0, t) &= 0 \\
N(L, t) &= +N_{r2}(t) & \text{or} & & u_0(L, t) &= 0 \\
M(0, t) &= -M_{r1}(t) & \text{or} & & w_0(0, t) &= 0 \\
M(L, t) &= +M_{r2}(t) & \text{or} & & w_0(L, t) &= 0 \\
Q(0, t) &= -Q_{r1}(t) - Pw'_0(0, t) & \text{or} & & \theta(0, t) &= 0 \\
Q(L, t) &= +Q_{r2}(t) - Pw'_0(L, t) & \text{or} & & \theta(L, t) &= 0
\end{aligned} \tag{3.69}$$

The Eq.(3.68) considers the coupling between shear, flexural and axial displacement which are due to the axial-flexural displacement coupling with the non-coincidence of elastic axis and mass axis.

By equating the viscous damping coefficient to zero ($c_1=c_2=c_3=0$) and constant axial force to zero ($P=0$), the Eq.(3.68) reduces into the equation which has been used by Ruotolo [24], Mahapatra and Gopalakrishnan [22] and Chakraborty et al.. Dong et al. [9], Palacz et al. [10], Abramovitch [30], Chandrashekhar et al. [8], Chen and Yang [6] and Mahapatra and Gopalakrishnan [4] used the equation by assuming the mid-plane symmetry ($\rho R=0$) and neglecting the axial displacement. Thus, in our study the derived equation of the motion is more generic which covered almost all the Timoshenko beam models. Regarding the effect of force, displacement approaches Ruotolo [24] and Mahapatra and Gopalakrishnan [22] in their previous studies, developed the axial-flexural-shear coupled composite beam model by considering no axial force and no viscous damping coefficient. In the present work the variational approach has been used to formulate the spectral element by considering the effect of axial forces and viscous damping.

3.5 Dynamics of Axial-Bending-Shear Coupled Composite Beams

3.5.1 Equation of Motion

The equations of motion with associated boundary condition derived in the previous section are given by,

$$\begin{aligned}
EA_e u_0'' - K_a \theta'' - \rho A_e \ddot{u}_0 + \rho R_e \ddot{\theta} - c_1 \dot{u}_0 + f_u(x, t) &= 0 \\
\kappa GA_e (w_0'' - \theta') + P w_0'' - \rho A_e \ddot{w}_0 - c_2 \dot{w}_0 + f_w(x, t) &= 0 \\
EI_e \theta'' + \kappa GA_e (w_0' - \theta) - K_a u_0'' + \rho R_e \ddot{u}_0 - \rho I_e \ddot{\theta} - c_3 \dot{\theta} + f_\theta(x, t) &= 0 \quad (3.70)
\end{aligned}$$

and

$$\begin{aligned}
N(0, t) &= -N_{r1}(t) \quad or \quad u_0(0, t) = 0 \\
N(L, t) &= +N_{r2}(t) \quad or \quad u_0(L, t) = 0 \\
M(0, t) &= -M_{r1}(t) \quad or \quad w_0(0, t) = 0 \\
M(L, t) &= +M_{r2}(t) \quad or \quad w_0(L, t) = 0 \\
Q(0, t) &= -Q_{r1}(t) - P w_0'(0, t) \quad or \quad \theta(0, t) = 0 \\
Q(L, t) &= +Q_{r2}(t) - P w_0'(L, t) \quad or \quad \theta(L, t) = 0 \quad (3.71)
\end{aligned}$$

where M is the resultant moment, N is the resultant axial force and Q is the resultant transverse shear force which are given by,

$$\begin{aligned}
M(x, t) &= EI_e \theta' - K_a u' \\
Q(x, t) &= \kappa GA_e (w' - \theta) \\
N(x, t) &= EA_e u' - K_a \theta' \quad (3.72)
\end{aligned}$$

3.5.2 Spectral Element Modeling

3.5.2.1 Formulation of Governing equations of motion in frequency domain

The displacement fields (of finite element) in the spectral form are assumed as,

$$\{w_0(x, t), u_0(x, t), \theta_0(x, t)\} = \frac{1}{N} \sum_{m=0}^{N-1} \{W_m(x; \omega_m), U_m(x; \omega_m), \Theta_m(x; \omega_m)\} e^{i\omega_m t} \quad (3.73)$$

where

N = sampling number

ω_n = discrete frequency given by $\omega_m = 2\pi m/T$ where $(m = 1, 2, \dots, N)$

and T is further depend upon N by DFT theory.

Now, $N = 2f_q T$, where f_q is the Nyquist frequency. Similarly all forces and moments can be represented in spectral form as:

$$\begin{aligned} \{f_w(x, t), f_u(x, t), f_\theta(x, t)\} &= \frac{1}{N} \sum_{m=0}^{N-1} \{F_{wm}(x; \omega_m), F_{um}(x; \omega_m), F_{\theta m}(x; \omega_m)\} e^{i\omega_m t} \\ \{M(x, t), N(x, t), Q(x, t)\} &= \frac{1}{N} \sum_{m=0}^{N-1} \{M_m(x; \omega_m), N_m(x; \omega_m), Q_m(x; \omega_m)\} e^{i\omega_m t} \\ \{M_{br}(t), N_{br}(t), Q_{br}(t)\} &= \frac{1}{N} \sum_{m=0}^{N-1} \{M_{brm}(x; \omega_m), N_{brm}(x; \omega_m), Q_{brm}(x; \omega_m)\} e^{i\omega_m t} \end{aligned} \quad (3.74)$$

where $(r = 1, 2)$

The term with subscript 'n' represent the Fourier components or spectral component of the related function element. Now by substituting the Eq.(3.73) and Eq.(3.74) into Eq.(3.70) and Eq.(3.71) and solving, the frequency domain

governing equation of motion with boundary conditions are given by

$$\begin{aligned}
EA_e U'' - K_a \Theta'' + \omega^2 \rho A_e U - \omega^2 \rho R_e \Theta - i\omega c_1 U + F_u &= 0 \\
\kappa GA_e (W'' - \Theta') + PW'' + \omega^2 \rho A_e W - i\omega c_2 W + F_w &= 0 \\
EI_e \Theta'' + \kappa GA_e (W' - \Theta) - K_a U'' - \omega^2 \rho R_e U + \omega^2 \rho I_e \Theta - i\omega c_3 \Theta + F_\theta &= 0 \quad (3.75)
\end{aligned}$$

and

$$\begin{aligned}
N(0) &= -N_{r1} & \text{or} & & U(0) &= 0 \\
N(L) &= +N_{r2} & \text{or} & & U(L) &= 0 \\
M(0) &= -M_{r1} & \text{or} & & W(0) &= 0 \\
M(L) &= +M_{r2} & \text{or} & & W(L) &= 0 \\
Q(0) &= -Q_{r1} - PW'(0) & \text{or} & & \Theta(0) &= 0 \\
Q(L) &= +Q_{r2} - PW'(L) & \text{or} & & \Theta(L) &= 0 \quad (3.76)
\end{aligned}$$

$$\begin{aligned}
M(x) &= EI_e \Theta' - K_a U' \\
Q(x) &= \kappa GA_e (W' - \Theta) \\
N(x) &= EA_e U' - K_a \Theta' \quad (3.77)
\end{aligned}$$

3.5.2.2 Spectral Nodal DOFs, Forces, and Moments

From Fig.(3.4) and Fig.(3.5) the spectral component of Forces, Moments and spectral nodal DOFs vector are define by

$$\begin{aligned}
\mathbf{d} &= \{U_1 \quad W_1 \quad \Theta_1 \quad U_2 \quad W_2 \quad \Theta_2\}^T \\
&= \{U(0) \quad W(0) \quad \Theta(0) \quad U(l) \quad W(l) \quad \Theta(l)\}^T \quad (3.78)
\end{aligned}$$

$$= \{N_1 \quad Q_1 \quad M_1 \quad N_2 \quad Q_2 \quad M_2\}^T \quad (3.79)$$

3.5.2.3 Dynamic shape functions

In the formulation of spectral element the spectral element model has been formulated with the use of frequency dependent dynamic shape function. Now the dynamic shape function can be derived from Eq.(3.75) as

$$\begin{aligned}
\kappa GA_e(W'' - \Theta') + PW'' + \omega^2 \rho A_2 W - i\omega c_2 W &= 0 \\
EI_e \Theta'' + \kappa GA_e(w' - \Theta) - K_a U'' - \omega^2 \rho R_e U + \omega^2 \rho I_e \Theta - i\omega c_3 \Theta &= 0 \\
EA_e U'' - K_a \Theta'' + \omega^2 \rho A_e U - \omega^2 \rho R_e \Theta - i\omega c_1 U &= 0
\end{aligned} \tag{3.80}$$

Now the general solution of Eq.(3.80) are assumed as:

$$W(x) = ae^{-ikx}, \quad \Theta(x) = \alpha ae^{-ikx}, \quad U(x) = \beta ae^{-ikx} \tag{3.81}$$

Substituting the general solution from Eq.(3.81) into Eq.(3.80) gives an eigenvalue problem as follows:

$$\begin{bmatrix} X_{11} & X_{12} & 0 \\ -X_{21} & X_{22} & X_{23} \\ 0 & X_{32} & X_{33} \end{bmatrix} \begin{Bmatrix} 1 \\ \alpha \\ \beta \end{Bmatrix} = \begin{Bmatrix} 0 \\ 0 \\ 0 \end{Bmatrix} \tag{3.82}$$

where

$$\begin{aligned}
X_{11} &= -(\kappa GA_e + P)k^2 + \omega^2 \rho A_e - i\omega c_2 \\
X_{12} &= X_{21} = +i\kappa GA_e k \\
X_{22} &= -EI_e k^2 - i\omega c_3 + \omega^2 \rho I_e - \kappa GA_e \\
X_{23} &= X_{32} = -\omega^2 \rho R_e + K_a k^2 \\
X_{33} &= \omega^2 \rho A_e - EA_e k^2 - i\omega c_1
\end{aligned} \tag{3.83}$$

By solving Eq.(3.82) the dispersion relation can be written as:

$$a_1 k_n^6 + a_2 k_n^4 + a_3 k_n^2 + a_4 = 0 \quad (3.84)$$

where($n = 1, 2, \dots, N$)

and

$$\begin{aligned} a_1 &= -(EA_e EI_e - K_a^2)(P + \kappa GA_e) \\ a_2 &= [-\rho A_e K_a^2 + (P + \kappa GA_e)(EI_e \rho A_e - 2\rho R_e K_a) \\ &\quad + EA_e(EI_e \rho A_e + \kappa GA_e \rho I_e + P \rho I_e)] \omega^2 \\ &\quad - [iEI_e(P + \kappa GA_e)c_1 + i(EA_e EI_e - K_a^2)c_2 \\ &\quad + iEA_e(P + \kappa GA_e)c_3] \omega - 2EA_e \kappa GA_e P \\ a_3 &= [-EA \rho A_e^2 - \kappa GA_e \rho A_e \rho I_e + 2K_a \rho A_e \rho R_e + \kappa GA_e \rho R_e^2 \\ &\quad - EA_e \rho A_e \rho I_e + P(\rho R_e^2 - \rho A_e \rho I_e)] \omega^4 + i [(EI_e \rho A_e \\ &\quad + P \rho I_e + \kappa GA_e \rho I_e) c_1 - (2K_a \rho R_e - EI_e \rho A_e - EA_e \rho I_e) c_2 \\ &\quad + \rho A_e (EA_e + P + \kappa GA_e) c_3] \omega^3 + [EI_e c_1 c_2 + (P + \kappa GA_e) \\ &\quad c_1 c_3 + EA_e c_2 c_3 + P \kappa GA_e \rho A_e] \omega^2 - i (P \kappa GA_e c_1 \\ &\quad + EA_e \kappa GA_e c_2) \omega + EA_e \kappa GA_e \rho A_e \\ a_4 &= (\rho A_e^2 \rho I_e - \rho A_e \rho R_e^2) \omega^6 - [i \rho A_e \rho I_e c_1 \\ &\quad + i(\rho A_e \rho I_e - \rho R_e^2) c_2 + i \rho A_e^2 c_3] \omega^5 - (\kappa GA_e \rho A_e^2 + \rho I_e c_1 c_2 \\ &\quad + \rho A_e c_1 c_3 + \rho A_e c_2 c_3) \omega^4 + (i \kappa GA_e \rho A_e c_1 - i \kappa GA_e \rho A_e c_2 \\ &\quad - i c_1 c_2 c_3) \omega^3 + \kappa GA_e c_1 c_2 \omega^2 \end{aligned} \quad (3.85)$$

The six wavenumbers can be obtain from the Eq.(3.85)

$$\begin{aligned} k_{1,2} &= \pm \sqrt{X_3 + X_4 - \frac{1}{3}(a_2/a_1)} \\ k_{3,4} &= \pm \sqrt{-\frac{1}{2}(X_3 + X_4) - \frac{1}{3}(a_2/a_1) + i \frac{\sqrt{3}}{2}(X_3 - X_4)} \\ k_{5,6} &= \pm \sqrt{-\frac{1}{2}(X_3 + X_4) - \frac{1}{3}(a_2/a_1) - i \frac{\sqrt{3}}{2}(X_3 - X_4)} \end{aligned} \quad (3.86)$$

where

$$\begin{aligned}
X_1 &= \frac{1}{9} [3(c_3/c_1) - (c_2/c_1)^2] \\
X_2 &= \frac{1}{54} [9(a_2a_3/a_1^2) - 27(a_4/a_1) - 2(a_2/a_1)^3] \\
X_3 &= \sqrt[3]{X_2 + \sqrt{X_1^3 + X_2^2}} \\
X_4 &= \sqrt[3]{X_2 - \sqrt{X_1^3 + X_2^2}}
\end{aligned} \tag{3.87}$$

Now by substituting the six wavenumbers k_p ($p = 1, 2, \dots, 6$) into Eq.(3.82), we have the corresponding six α_p and β_p ($p = 1, 2, \dots, 6$) given by,

$$\begin{aligned}
\alpha_p &= i \frac{\omega^2 \rho A_e - \kappa G A_e k_p^2 - P k_p^2}{\kappa G A_e k_p} \\
\beta_p &= \left(\frac{\omega^2 \rho R_e - K_a k_p^2}{\omega^2 \rho A_e - E A_e k_p^2} \right) \alpha_p
\end{aligned} \tag{3.88}$$

Now by using this six wavenumbers from Eq.(3.86) the genral solution of Eq.(3.80) can be written as:

$$\begin{aligned}
W(x) &= \sum_{p=1}^6 a_p e^{ik_p x} \\
U(x) &= \sum_{p=1}^6 \beta_p b_p e^{-ik_p x} \\
\Theta(x) &= \sum_{p=1}^6 \alpha_p a_p e^{-ik_p x}
\end{aligned} \tag{3.89}$$

or

$$\begin{aligned}
W(x) &= \mathbf{e}(x; \omega) \mathbf{a} \\
U(x) &= \mathbf{e}(x; \omega) \mathbf{B}(\omega) \mathbf{a} \\
\Theta(x) &= \mathbf{e}(x; \omega) \mathbf{A}(\omega) \mathbf{a}
\end{aligned} \tag{3.90}$$

where

$$\mathbf{e}(x; \omega) = \begin{bmatrix} e^{-ik_1 x} & e^{-ik_2 x} & e^{-ik_3 x} & e^{-ik_4 x} & e^{-ik_5 x} & e^{-ik_6 x} \end{bmatrix} \tag{3.91}$$

and

$$\mathbf{a} = \left\{ a_1 \quad a_2 \quad a_3 \quad a_4 \quad a_5 \quad a_6 \right\}^T \quad (3.92)$$

$$\mathbf{A}(\omega) = \text{diag} [\alpha_p(\omega)]$$

$$\mathbf{B}(\omega) = \text{diag} [\beta_p(\omega)]$$

$$\text{where } (p = 1, 2, \dots, 6) \quad (3.93)$$

Using the spectral nodal DOFs given by Eq.(3.78) to Eq.(3.90), we have:

$$\mathbf{d} = \mathbf{H}(\omega)\mathbf{a} \quad (3.94)$$

where,

$$\mathbf{H}(\omega) = \begin{bmatrix} \beta_1 & \beta_2 & \beta_3 & \beta_4 & \beta_5 & \beta_6 \\ 1 & 1 & 1 & 1 & 1 & 1 \\ \alpha_1 & \alpha_2 & \alpha_3 & \alpha_4 & \alpha_5 & \alpha_6 \\ \beta_1 e_1 & \beta_2 e_2 & \beta_3 e_3 & \beta_4 e_4 & \beta_5 e_5 & \beta_6 e_6 \\ e_1 & e_2 & e_3 & e_4 & e_5 & e_6 \\ \alpha_1 e_1 & \alpha_2 e_2 & \alpha_3 e_3 & \alpha_4 e_4 & \alpha_5 e_5 & \alpha_6 e_6 \end{bmatrix} \quad (3.95)$$

with

$$e_p = e^{-ik_p L} \quad (p = 1, 2, \dots, 6) \quad (3.96)$$

With the help of Eq.(3.94) we can remove the constant vector \mathbf{a} from the Eq.(3.90) and write the general solution as,

$$\begin{aligned} W(x) &= \mathbf{N}_w(x; \omega)\mathbf{d} \\ U(x) &= \mathbf{N}_u(x; \omega)\mathbf{d} \\ \Theta(x) &= \mathbf{N}_\theta(x; \omega)\mathbf{d} \end{aligned} \quad (3.97)$$

where N_w, N_u and N_θ are the three dynamic shape function which are given as

$$\begin{aligned} \mathbf{N}_w(x; \omega_n) &= \mathbf{e}(x; \omega_n)\mathbf{H}^{-1}(\omega) \\ \mathbf{N}_u(x; \omega_n) &= \mathbf{e}(x; \omega_n)\mathbf{B}(\omega)\mathbf{H}^{-1}(\omega) \\ \mathbf{N}_\theta(x; \omega_n) &= \mathbf{e}(x; \omega_n)\mathbf{A}(\omega)\mathbf{H}^{-1}(\omega) \end{aligned} \quad (3.98)$$

3.5.2.4 Weak Form of frequency domain Governing Equations

The frequency domain governing differential equation is in the form of pseudo-static problem, thus the weak form of governing equation can be derived from the Eq.(3.71). This weak form of frequency domain governing equation is used for formulating the spectral element equation, which can be obtained from Eq.(3.75) as,

$$\begin{aligned}
& \int_0^L \{ [\kappa G A_e (W'' - \Theta') + P W'' + \omega^2 \rho A_e W - i \omega c_2 W + F_w] \delta W \\
& + [E A_e U'' - K_a \Theta'' + \omega^2 \rho A_e U - \omega^2 \rho R_e \Theta - i \omega c_1 U + F_u] \delta U \\
& + [E I_e \Theta'' + \kappa G A_e (W' - \Theta) - K_a U'' - \omega^2 \rho R_e U + \omega^2 \rho I_e \Theta \\
& - i \omega c_3 \Theta + F_\theta] \delta \Theta \} dx = 0
\end{aligned} \tag{3.99}$$

Now by applying integral by parts to Eq.(3.99) and then using the force-displacement relationship from Eq.(3.71), the weak form can be derive as:

$$\begin{aligned}
& \int_0^L \{ - \kappa G A_e W' \delta W' + \kappa G A_e (\Theta \delta W' + W' \delta \Theta) - \kappa G A_e \Theta \delta \Theta \\
& - E I_e \Theta' \delta \Theta' - E A_e U' \delta U' + K_a (U' \delta \Theta' + \Theta' \delta U') - P W' \delta W' \\
& + \omega^2 \rho A_e U \delta U + \omega^2 \rho A_e W \delta W + \omega^2 \rho I_e \Theta \delta \Theta - \omega^2 \rho R_e U \delta \Theta \\
& - \omega^2 \rho R_e \Theta \delta U - i \omega c_1 U \delta U - i \omega c_2 W \delta W - i \omega c_3 \Theta \delta \Theta + F_u \delta U \\
& + F_w \delta W + F_\theta \delta \Theta \} dx + N(x) \delta U|_0^L + M(x) \delta \Theta|_0^L \\
& + [Q(x) + P W'] \delta W|_0^L
\end{aligned} \tag{3.100}$$

or applying the boundary condition to Eq.(3.76), Eq.(3.78) and Eq.(3.79)

$$\int_0^L \{ \kappa GA_e W' \delta W' - \kappa GA_e (\Theta \delta W' + w' \delta \Theta) + \kappa GA_e \Theta \delta \Theta \quad (3.101)$$

$$\begin{aligned} &+ EI_e \Theta' \delta \Theta' + EA_e U' \delta U' - K_a (U' \delta \Theta' + \Theta' \delta U') + PW' \delta W' \\ &- \omega^2 \rho A_e U \delta U - \omega^2 \rho A_e W \delta W - \omega^2 \rho I_e \Theta \delta \Theta + \omega^2 \rho R_e U \delta \Theta \\ &+ \omega^2 \rho R_e \Theta \delta U + i\omega c_1 U \delta U + i\omega c_2 W \delta W + i\omega c_3 \Theta \delta \Theta \} dx \\ &= \delta \mathbf{d}^T \mathbf{f}_c + \int_0^L (F_u \delta U + F_w \delta W + F_\theta \delta \Theta) dx \quad (3.102) \end{aligned}$$

3.5.2.5 Formulation of Spectral Element Equation

Substituting the Eq.(3.97) into Eq.(3.102), we have

$$\begin{aligned} \delta \mathbf{d}^T \int_0^L \{ &\kappa GA_e N_w'^T N_w' - \kappa GA_e (N_w'^T N_\theta' + N_\theta'^T N_w') + \kappa GA_e N_\theta'^T N_\theta \\ &+ EI_e N_\theta'^T N_\theta' + EA_e N_u'^T N_u' - K_a (N_\theta'^T N_u' + N_u'^T N_\theta') \\ &+ P N_w'^T N_w' - \omega^2 \rho A_e (N_u^T N_u + N_w^T N_w) - \omega^2 \rho I_e N_\theta'^T N_\theta \\ &+ i\omega c_1 N_u'^T N_u + i\omega c_2 N_w'^T N_w + i\omega c_3 N_\theta'^T N_\theta \\ &+ \omega^2 \rho R_e (N_\theta^T N_u + N_u^T N_\theta) \} dx \mathbf{d} = \delta^T (f_c + f_d) \quad (3.103) \end{aligned}$$

where

$$\mathbf{f}_d = \int_0^L (F_u N_u^T + F_w N_w^T + F_\theta N_\theta^T) dx \quad (3.104)$$

In the above equation $\delta \mathbf{d}$ is virtual displacement which is arbitrary by definition, Thus the spectral element equation can be obtain by Eq.(3.103) as

$$\mathbf{S}(\omega) \mathbf{d} = \mathbf{f}_c + \mathbf{f}_d \quad (3.105)$$

where $\mathbf{S}(\omega)$ is a frequency dependent six-by-six spectral element matrix which is given by,

$$\begin{aligned}
\mathbf{S}(\omega) = \int_0^L \{ & \kappa G A_e N_w'^T N_w' - \kappa G A_e (N_w'^T N_\theta' + N_\theta'^T N_w') + \kappa G A_e N_\theta'^T N_\theta' \\
& + E I_e N_\theta'^T N_\theta' + E A_e N_u'^T N_u' - K_a (N_\theta'^T N_u' + N_u'^T N_\theta') \\
& + P N_w'^T N_w' - \omega^2 \rho A_e (N_u^T N_u + N_w^T N_w) - \omega^2 \rho I_e N_\theta'^T N_\theta' \\
& + i\omega c_1 N_u^T N_u + i\omega c_2 N_w^T N_w + i\omega c_3 N_\theta'^T N_\theta' \\
& + \omega^2 \rho R_e (N_\theta^T N_u + N_u^T N_\theta) \} dx \tag{3.106}
\end{aligned}$$

By putting Eq.(3.98) into Eq.(3.106), the spectral element matrix can be expressed as follows,

$$\mathbf{S}(\omega) = \mathbf{H}^{-T}(\omega) \mathbf{D}(\omega) \mathbf{H}^{-1}(\omega) \tag{3.107}$$

where

$$\begin{aligned}
\mathbf{D}(\omega) = \int_0^L [& \kappa G A_e e'^T e' - \kappa G A_e (e'^T e B + B^T e^T e') + \kappa G A_e B^T e^T e B \\
& + E I_e B^T e'^T e' B + E A_e A^T e'^T e' A - K_a (B^T e'^T e' A + A^T e'^T e' B) \\
& + P e'^T e' - \omega^2 \rho A_e (A^T e^T e A + e^T e) - \omega^2 \rho I_e B^T e^T e B \\
& + i\omega (c_1 A^T e^T e A + c_2 e^T e + c_3 B^T e^T e B) \\
& + \omega^2 \rho R_e (B^T e^T e A + A^T e^T e B)] dx \tag{3.108}
\end{aligned}$$

The derivative of $\mathbf{e}(x; \omega)$ with respect to x can be obtain from Eq.(3.91) as

$$\mathbf{e}'(x; \omega) = -i\mathbf{e}(x; \omega) \mathbf{K}(\omega) \tag{3.109}$$

where

$$\mathbf{K} = \text{diag} [k_p] \quad (p = 1, 2, \dots, 6) \tag{3.110}$$

Substituting the Eq.(3.91) and Eq.(3.109) into Eq.(3.108) gives,

$$\begin{aligned}
\mathbf{D}(\omega) = & \kappa G A_e [-\mathbf{K}\mathbf{E}\mathbf{K} + i(\mathbf{K}\mathbf{E}\mathbf{B} + \mathbf{B}^T\mathbf{E}\mathbf{K}) + \mathbf{B}^T\mathbf{E}\mathbf{B}] \\
& - E I_e \mathbf{B}^T \mathbf{K} \mathbf{E} \mathbf{K} \mathbf{B} - E A_e \mathbf{A}^T \mathbf{K} \mathbf{E} \mathbf{K} \mathbf{A} + K_a (\mathbf{B}^T \mathbf{K} \mathbf{E} \mathbf{K} \mathbf{A} \\
& + \mathbf{A}^T \mathbf{K} \mathbf{E} \mathbf{K} \mathbf{B}) - P \mathbf{K} \mathbf{E} \mathbf{K} - \omega^2 [\rho A_e (\mathbf{A}^T \mathbf{E} \mathbf{A} + \mathbf{E}) \\
& + \rho I_e \mathbf{B}^T \mathbf{E} \mathbf{B} - \rho R_e (\mathbf{B}^T \mathbf{E} \mathbf{A} + \mathbf{A}^T \mathbf{E} \mathbf{B})] + i\omega (c_1 \mathbf{A}^T \mathbf{E} \mathbf{A} \\
& + c_2 \mathbf{E} + c_3 \mathbf{B}^T \mathbf{E} \mathbf{B})
\end{aligned} \tag{3.111}$$

where

$$\mathbf{E}(\omega) = \int_0^L \mathbf{e}^T(x; \omega) \mathbf{e}(x; \omega) dx = [E_{rs}(\omega)] \quad (r, s = 1, 2, \dots, 6) \tag{3.112}$$

with

$$E_{rs} = \begin{cases} \frac{i}{k_r + k_s} [e^{-i(k_r + k_s)L} - 1] & \text{if } k_r + k_s \neq 0 \\ L & \text{if } k_r + k_s = 0 \end{cases} \tag{3.113}$$

3.5.3 Spectral Element Analysis

The spectral element or spectrally formulated finite elements given by Eq.(3.113) are assembled in purely analogous way as conventionally used in finite element method. Now applying the boundary condition and assembling into the global form, the global spectral element can be find out by

$$\mathbf{S}_g(\omega) \mathbf{d}_g = \mathbf{f}_g(\omega) \tag{3.114}$$

where

$\mathbf{S}_g(\omega)$ = Global dynamic stiffness matrix or global spectral matrix,

\mathbf{d}_g = Global spectral nodal DOFs vector,

\mathbf{f}_g = Global spectral nodal forces vector,

The natural frequencies ω_{nat} can be obtained by equating the determinant of $\mathbf{S}_g = 0$. Now,

$$\det \mathbf{S}(\omega_{nat}) = 0 \tag{3.115}$$

Chapter 3 *Spectral Element model for Composite Timoshenko Beam*

Similarly six wave-numbers k_i ($i = 1, 2, \dots, 6$) can be obtained corresponding to each natural frequency from the dispersion relation Eq.(3.84).

Chapter 4

Numerical Results and Discussion

4.1 Natural frequencies of a symmetrical laminated composite beam with different boundary conditions

The natural frequencies of the free vibration of composite laminated beam with uniform cross-section under different boundary conditions are computed using SEM considering all the effects of axial-bending-shear coupled and decoupled forces.

To study the present spectral element model we have considered a cross ply composite laminated beam. There are four layer in this beam similar to that considered in the study of Chandrashekhara et al. [8]. AS/3501-6 graphite epoxy material is used in each layer of the composite beam with orientation as

$[0^\circ/90^\circ/90^\circ/0^\circ]$. Its material properties are given as:

$$E_1 = 144.84 \text{ GPa},$$

$$E_2 = 9.65 \text{ GPa},$$

$$G_{12} = G_{31} = 4.14 \text{ GPa},$$

$$G_{23} = 3.45 \text{ GPa},$$

$$\nu_{12} = 0.3,$$

$$\nu_{21} = 0.02,$$

$$\rho = 1389.79 \text{ kg/m}^3$$

$$L = 0.381\text{m} \text{ (Length)}$$

$$h = 0.0254\text{m} \text{ (Thickeness)}$$

$$b = 0.0254\text{m} \text{ (width)}$$

$$\kappa = 5/6 \text{ (shear correction factor)}$$

Table 4.1 to 4.5 shows the comparison of natural frequencies of non-dimensional characteristics for a symmetrical $[0/90/90/0]$ cross-ply composite beam subjected to different boundary conditions. The Table 4.6 to 4.20 shows the comparison of fundamental natural frequencies of non-dimensional characteristics for a symmetrical $[+\phi/-\phi/-\phi/+\phi]$ cross-ply composite beams subjected to various boundary condition such as the clamped-free (CF), clamped-clamped (CC), clamped-simply supported (CS), simply-simply supported (SS) and free-free (FF) boundary condition. The different values of ϕ are 15° , 30° , and 45° . The results of present SEM model with a single element exactly matches with that of Chandrashekhara et al. [8] with 150 elements. As the number of elements used in FEM analysis is increased, the FEM results indeed converge to the present SEM results.

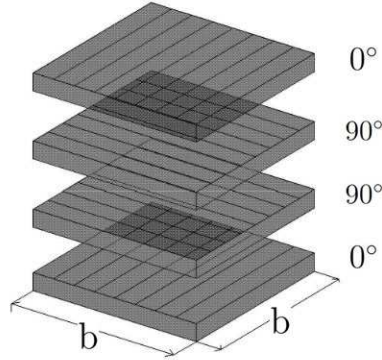


Figure 4.1: Symmetrical cross-ply orientation $[0^\circ/90^\circ/90^\circ/0^\circ]$

4.1.1 $[0^\circ/90^\circ/90^\circ/0^\circ]$ Ply Oriented Beam

Fig.(4.1) shows the orientation of the symmetrical cross-ply. Table 4.1 to 4.5 provide the comparison between present SEM model and past FEM analysis of non dimensional natural frequencies ($\bar{\omega} = \omega L^2 \sqrt{\rho/(E_1 h^2)}$) for the $[0^\circ/90^\circ/90^\circ/0^\circ]$ cross-ply symmetrical composite beams subjected to various boundary condition such as the simply-simply supported (SS) clamped-free (CF), clamped-clamped (CC), clamped-simply supported (CS) and free-free (FF) boundary condition respectively. The material properties are taken as $E_1 = 144.84 \text{ GPa}$, $E_2 = 9.65 \text{ GPa}$, $G_{12} = G_{31} = 4.14 \text{ GPa}$, $G_{23} = 3.45 \text{ GPa}$, $\nu_{12} = .3$, $\nu_{21} = 0.02$, $\rho = 1389.79 \text{ kg/m}^3$

Table 4.1: Comparison of non-dimensional natural frequencies for a symmetrical $[0^\circ/90^\circ/90^\circ/0^\circ]$ angle-ply simply supported composite beam

| Mode | SEM(m) | FEM(m) | | | | | | Chandrashekhara et al. [8] |
|----------------|------------|------------|----------|----------|----------|-----------|-----------|-------------------------------|
| | $m = 1$ | $m = 2$ | $m = 10$ | $m = 30$ | $m = 50$ | $m = 100$ | $m = 150$ | |
| 1 | 2.502 | 2.542 | 2.504 | 2.503 | 2.502 | 2.502 | 2.502 | 2.502 |
| 2 | 8.481 | 11.84 | 8.534 | 8.488 | 8.484 | 8.481 | 8.481 | 8.481 |
| 3 | 15.76 | 28.46 | 16.09 | 15.79 | 15.77 | 15.76 | 15.76 | 15.76 |
| 4 | 23.31 | 38.06 | 24.38 | 23.43 | 23.36 | 23.32 | 23.32 | 23.31 |
| 5 | 30.84 | 64.81 | 33.31 | 31.12 | 30.94 | 30.87 | 30.86 | 30.86 |
| 6 ^b | 34.52 | 76.12 | 34.66 | 34.53 | 34.52 | 34.52 | 34.52 | - |
| 7 | 38.29 | 75.64 | 41.56 | 39.74 | 38.69 | 38.29 | 38.29 | 38.29 |
| 8 | 45.65 | - | 51.15 | 47.85 | 46.09 | 45.87 | 45.65 | 45.65 |
| 9 | 52.94 | - | 55.65 | 54.48 | 53.01 | 52.96 | 52.94 | 52.94 |
| 10 | 60.18 | - | 70.18 | 62.23 | 60.91 | 60.35 | 60.25 | 60.18 |
| 20 | 117.0 | - | 221.4 | 122.4 | 118.3 | 117.2 | 117.2 | 117.0 |

m = element numbers used in SEM & FEM analysis,

b = Axial modes

Table 4.2: Comparison of non-dimensional natural frequencies for a symmetrical $[0^\circ/90^\circ/90^\circ/0^\circ]$ angle-ply cantilevered composite beam

| Mode | SEM(m) | FEM(m) | | | | | | Chandrashekhara et al. [8] |
|-----------------|------------|------------|----------|----------|----------|-----------|-----------|-------------------------------|
| | $m = 1$ | $m = 2$ | $m = 10$ | $m = 30$ | $m = 50$ | $m = 100$ | $m = 150$ | |
| 1 | 0.924 | 0.926 | 0.924 | 0.924 | 0.924 | 0.924 | 0.924 | 0.924 |
| 2 | 4.893 | 5.068 | 4.895 | 4.894 | 4.893 | 4.893 | 4.893 | 4.893 |
| 3 | 11.44 | 17.71 | 11.47 | 11.46 | 11.45 | 11.44 | 11.44 | 11.44 |
| 4 ^b | 17.26 | 19.03 | 17.26 | 17.26 | 17.26 | 17.26 | 17.26 | - |
| 5 | 18.70 | 52.92 | 18.84 | 18.76 | 18.72 | 18.71 | 18.70 | 18.70 |
| 6 | 26.21 | 61.85 | 26.59 | 26.38 | 26.28 | 26.23 | 26.21 | 26.21 |
| 7 | 33.72 | - | 41.56 | 39.74 | 38.69 | 35.76 | 33.42 | 33.72 |
| 8 | 41.17 | - | 51.15 | 47.85 | 46.09 | 45.87 | 41.93 | 41.17 |
| 9 | 48.54 | - | 55.65 | 54.48 | 53.01 | 52.96 | 49.03 | 48.54 |
| 10 ^b | 51.78 | - | 51.90 | 51.83 | 51.80 | 51.78 | 51.78 | - |
| 20 | 117.2 | - | 122.3 | 120.0 | 118.9 | 118.2 | 117.6 | 117.2 |

m = element numbers used in SEM & FEM analysis,

b = Axial modes

Table 4.3: Comparison of non-dimensional natural frequencies for a symmetrical $[0^\circ/90^\circ/90^\circ/0^\circ]$ angle-ply clamped-clamped composite beam

| Mode | SEM(m) | FEM(m) | | | | | | | Chandrashekhara et al. [8] |
|------|------------|------------|----------|----------|----------|-----------|-----------|-----------|-------------------------------|
| | $m = 1$ | $m = 2$ | $m = 10$ | $m = 30$ | $m = 50$ | $m = 100$ | $m = 150$ | $m = 200$ | |
| 1 | 4.594 | 4.561 | 4.573 | 4.591 | 4.594 | 4.594 | 4.594 | 4.594 | 4.594 |
| 2 | 16.97 | 17.91 | 17.56 | 17.36 | 17.13 | 17.02 | 16.97 | 16.97 | 16.97 |
| 3 | 31.30 | 33.28 | 33.15 | 33.06 | 32.54 | 31.90 | 31.51 | 31.30 | 31.30 |
| 4 | 45.84 | 47.21 | 47.06 | 46.79 | 46.15 | 46.03 | 45.91 | 45.84 | 45.84 |
| 5 | 60.25 | 64.59 | 63.91 | 63.08 | 62.37 | 61.88 | 60.93 | 60.33 | 60.25 |
| 6 | 74.55 | 76.88 | 76.56 | 75.93 | 75.07 | 74.89 | 74.66 | 74.59 | 74.55 |
| 7 | 88.75 | 93.71 | 91.30 | 90.75 | 89.46 | 89.12 | 88.92 | 88.81 | 88.75 |
| 8 | 102.90 | - | 109.56 | 107.29 | 105.43 | 104.22 | 103.09 | 103.01 | 102.90 |
| 9 | 117.00 | - | 123.85 | 121.56 | 120.97 | 119.08 | 118.64 | 117.34 | 117.00 |
| 10 | 124.14 | - | 131.63 | 129.84 | 127.85 | 126.40 | 125.47 | 124.62 | 124.14 |
| 20 | 243.03 | - | 264.26 | 257.19 | 251.91 | 247.71 | 244.72 | 243.84 | 243.03 |

m = element numbers used in SEM & FEM analysis

Table 4.4: Comparison of non-dimensional natural frequencies for a symmetrical $[0^\circ/90^\circ/90^\circ/0^\circ]$ angle-ply clamped-simply supported composite beam

| Mode | SEM(m) | FEM(m) | | | | | | | Chandrashekhara et al. [8] |
|------|------------|------------|----------|----------|----------|-----------|-----------|-----------|-------------------------------|
| | $m = 1$ | $m = 2$ | $m = 10$ | $m = 30$ | $m = 50$ | $m = 100$ | $m = 150$ | $m = 200$ | |
| 1 | 3.525 | 3.598 | 3.581 | 3.549 | 3.525 | 3.525 | 3.525 | 3.525 | 3.525 |
| 2 | 9.44 | 9.71 | 9.69 | 9.51 | 9.49 | 9.47 | 9.44 | 9.44 | 9.44 |
| 3 | 16.39 | 18.06 | 17.92 | 17.64 | 17.19 | 16.73 | 16.41 | 16.39 | 16.39 |
| 4 | 23.69 | 25.46 | 25.13 | 24.88 | 24.39 | 24.03 | 23.85 | 23.69 | 23.70 |
| 5 | 31.07 | 33.74 | 33.16 | 32.57 | 32.09 | 31.81 | 31.42 | 31.11 | 31.07 |
| 6 | 38.43 | 49.81 | 46.78 | 44.19 | 41.97 | 40.26 | 39.05 | 38.88 | 38.43 |
| 7 | 45.74 | 58.41 | 55.76 | 51.91 | 49.18 | 47.01 | 46.17 | 45.92 | 45.74 |
| 8 | 52.99 | - | 67.66 | 63.42 | 59.19 | 57.49 | 54.81 | 53.34 | 53.00 |
| 9 | 60.21 | - | 81.21 | 75.43 | 71.94 | 67.19 | 63.82 | 61.07 | 60.22 |
| 10 | 67.38 | - | 89.43 | 82.51 | 76.47 | 72.34 | 69.18 | 67.44 | 67.38 |
| 20 | 133.37 | - | 148.72 | 141.81 | 137.89 | 135.97 | 134.71 | 133.43 | 133.37 |

m = element numbers used in SEM & FEM analysis

Table 4.5: Comparison of non-dimensional natural frequencies for a symmetrical $[0^\circ/90^\circ/90^\circ/0^\circ]$ angle-ply free-free composite beam

| Mode | SEM(m) | FEM(m) | | | | | | | Chandrashekara et al. [8] |
|------|------------|------------|----------|----------|----------|-----------|-----------|-----------|------------------------------|
| | $m = 1$ | $m = 2$ | $m = 10$ | $m = 30$ | $m = 50$ | $m = 100$ | $m = 150$ | $m = 200$ | |
| 1 | 5.55 | 5.583 | 5.581 | 5.549 | 5.525 | 5.525 | 5.525 | 5.525 | 5.55 |
| 2 | 12.76 | 12.81 | 12.79 | 12.79 | 12.79 | 12.78 | 12.77 | 12.77 | 12.76 |
| 3 | 20.69 | 23.41 | 22.35 | 21.10 | 20.75 | 20.73 | 20.73 | 20.70 | 20.69 |
| 4 | 25.14 | 29.46 | 28.13 | 27.88 | 27.39 | 27.03 | 26.85 | 26.69 | 25.14 |
| 5 | 36.33 | 45.74 | 43.16 | 42.57 | 41.09 | 39.81 | 37.42 | 37.11 | 36.33 |
| 6 | 43.89 | 57.81 | 55.78 | 53.19 | 49.97 | 48.26 | 46.05 | 44.88 | 43.89 |
| 7 | 51.30 | 60.41 | 58.76 | 56.91 | 56.18 | 55.01 | 53.17 | 51.92 | 51.30 |
| 8 | 56.51 | 69.70 | 67.66 | 63.42 | 59.19 | 57.49 | 54.81 | 53.34 | 56.51 |
| 9 | 62.50 | 83.63 | 81.21 | 75.43 | 71.94 | 67.19 | 64.82 | 63.07 | 62.50 |
| 10 | 70.01 | 97.26 | 95.43 | 92.51 | 86.47 | 82.34 | 79.18 | 74.41 | 70.01 |
| 20 | 80.27 | 99.92 | 98.72 | 91.81 | 87.89 | 85.97 | 84.71 | 83.43 | 80.27 |

m = element numbers used in SEM & FEM analysis

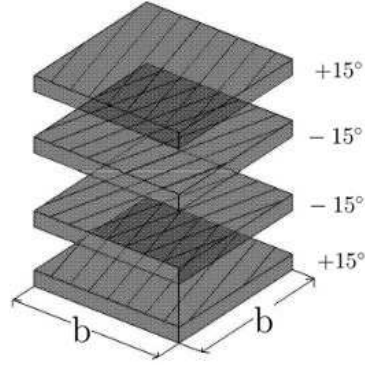


Figure 4.2: Symmetrical cross-ply orientation $[+15^\circ / -15^\circ / -15^\circ / +15^\circ]$

4.1.2 $[+15^\circ / -15^\circ / -15^\circ / +15^\circ]$ Ply Oriented Beam

Fig.(4.2) shows the orientation of the symmetrical cross-ply. Table 4.6 to 4.10 provide the comparison between present SEM model and past FEM analysis of non dimensional natural frequencies ($\bar{\omega} = \omega L^2 \sqrt{\rho / (E_1 h^2)}$) for the $[+15^\circ / -15^\circ / -15^\circ / +15^\circ]$ cross-ply symmetrical composite beams subjected to various boundary condition such as the simply-simply supported (SS) clamped-free (CF), clamped-clamped (CC), clamped-simply supported (CS) and free-free (FF) boundary condition respectively. The material properties are taken as $E_1 = 144.84 \text{ GPa}$, $E_2 = 9.65 \text{ GPa}$, $G_{12} = G_{31} = 4.14 \text{ GPa}$, $G_{23} = 3.45 \text{ GPa}$, $\nu_{12} = .3$, $\nu_{21} = 0.02$, $\rho = 1389.79 \text{ kg/m}^3$

Table 4.6: Comparison of non-dimensional natural frequencies for a symmetrical $[+15^\circ / -15^\circ / -15^\circ / +15^\circ]$ angle-ply simply supported composite beam

| Mode | SEM(m) | FEM(m) | | | | | | Chandrashekhara et al. [8] |
|------|------------|------------|----------|----------|----------|-----------|-----------|-------------------------------|
| | $m = 1$ | $m = 2$ | $m = 10$ | $m = 30$ | $m = 50$ | $m = 100$ | $m = 150$ | |
| 1 | 2.506 | 2.512 | 2.505 | 2.504 | 2.506 | 2.506 | 2.506 | 2.506 |
| 2 | 8.589 | 11.89 | 8.533 | 8.467 | 8.484 | 8.481 | 8.589 | 8.589 |
| 3 | 16.08 | 29.71 | 18.09 | 17.91 | 16.84 | 16.76 | 16.11 | 16.08 |
| 4 | 23.91 | 38.06 | 26.38 | 25.41 | 24.49 | 24.37 | 24.02 | 23.91 |
| 5 | 31.75 | 64.81 | 47.31 | 33.12 | 32.94 | 32.75 | 31.86 | 31.75 |
| 6 | 39.50 | 78.64 | 43.56 | 41.74 | 40.71 | 40.29 | 39.86 | 39.57 |
| 7 | 47.16 | - | 51.55 | 49.65 | 49.09 | 48.87 | 47.65 | 47.18 |
| 8 | 54.75 | - | 59.56 | 58.48 | 56.07 | 55.96 | 54.94 | 54.75 |
| 9 | 62.28 | - | 72.18 | 66.73 | 64.94 | 63.31 | 62.65 | 62.28 |
| 10 | 69.76 | - | 77.91 | 75.32 | 73.91 | 71.35 | 70.23 | 69.77 |
| 20 | 129.45 | - | 221.4 | 136.11 | 134.03 | 132.41 | 130.02 | 129.44 |

m = element numbers used in SEM & FEM analysis

Table 4.7: Comparison of non-dimensional natural frequencies for a symmetrical $[+15^\circ / -15^\circ / -15^\circ / +15^\circ]$ angle-ply cantilevered composite beam

| Mode | SEM(m) | FEM(m) | | | | | | Chandrashekhara et al. [8] |
|------|------------|------------|----------|----------|----------|-----------|-----------|-------------------------------|
| | $m = 1$ | $m = 2$ | $m = 10$ | $m = 30$ | $m = 50$ | $m = 100$ | $m = 150$ | |
| 1 | 0.924 | 0.926 | 0.924 | 0.924 | 0.924 | 0.924 | 0.924 | 0.924 |
| 2 | 4.946 | 5.068 | 4.895 | 4.894 | 4.893 | 4.893 | 4.893 | 4.893 |
| 3 | 11.649 | 17.471 | 12.047 | 11.946 | 11.874 | 11.710 | 11.681 | 11.649 |
| 4 | 19.14 | 52.92 | 18.84 | 18.76 | 18.72 | 18.71 | 18.70 | 19.14 |
| 5 | 26.93 | 61.85 | 26.59 | 26.38 | 26.28 | 26.23 | 26.21 | 26.93 |
| 6 | 34.73 | - | 41.56 | 39.74 | 38.69 | 35.76 | 33.42 | 34.73 |
| 7 | 42.48 | - | 51.15 | 47.85 | 46.09 | 45.87 | 41.93 | 42.48 |
| 8 | 50.15 | - | 55.65 | 54.48 | 53.01 | 52.96 | 49.03 | 50.15 |
| 9 | 57.75 | - | 51.90 | 51.83 | 51.80 | 51.78 | 51.78 | 57.75 |
| 10 | 65.28 | - | 73.90 | 71.83 | 70.80 | 69.78 | 67.78 | 65.28 |
| 20 | 131.59 | - | 134.37 | 133.84 | 132.96 | 132.42 | 131.6 | 131.59 |

m = element numbers used in SEM & FEM analysis

Table 4.8: Comparison of non-dimensional natural frequencies for a symmetrical $[+15^\circ / -15^\circ / -15^\circ / +15^\circ]$ angle-ply clamped-clamped composite beam

| Mode | SEM(m) | FEM(m) | | | | | | | Chandrashekhara et al. [8] |
|------|------------|------------|----------|----------|----------|-----------|-----------|-----------|-------------------------------|
| | $m = 1$ | $m = 2$ | $m = 10$ | $m = 30$ | $m = 50$ | $m = 100$ | $m = 150$ | $m = 200$ | |
| 1 | 4.663 | 4.561 | 4.573 | 4.591 | 4.594 | 4.594 | 4.594 | 4.594 | 4.663 |
| 2 | 17.41 | 18.91 | 18.56 | 18.26 | 17.91 | 17.41 | 17.41 | 17.41 | 17.41 |
| 3 | 32.26 | 35.13 | 34.15 | 33.08 | 32.54 | 32.90 | 32.26 | 32.26 | 32.26 |
| 4 | 47.38 | 54.21 | 52.06 | 50.79 | 49.85 | 49.03 | 48.91 | 47.38 | 47.39 |
| 5 | 62.38 | 66.91 | 66.63 | 65.08 | 64.47 | 63.88 | 62.93 | 62.39 | 62.38 |
| 6 | 77.26 | 87.05 | 85.52 | 83.96 | 80.07 | 79.89 | 78.66 | 77.59 | 77.27 |
| 7 | 92.03 | - | 103.36 | 101.73 | 98.46 | 94.13 | 93.92 | 92.88 | 92.03 |
| 8 | 106.74 | - | 109.61 | 108.39 | 107.13 | 106.22 | 105.09 | 106.91 | 106.74 |
| 9 | 121.39 | - | 123.85 | 123.56 | 122.97 | 122.06 | 122.64 | 121.94 | 121.39 |
| 10 | 128.77 | - | 131.63 | 131.14 | 130.85 | 130.50 | 129.74 | 129.02 | 128.77 |
| 20 | 252.36 | - | 259.11 | 257.86 | 256.19 | 254.91 | 253.27 | 252.84 | 252.36 |

m = element numbers used in SEM & FEM analysis

Table 4.9: Comparison of non-dimensional natural frequencies for a symmetrical $[+15^\circ / -15^\circ / -15^\circ / +15^\circ]$ angle-ply clamped-simply supported composite beam

| Mode | SEM(m) | FEM(m) | | | | | | | Chandrashekhara et al. [8] |
|------|------------|------------|----------|----------|----------|-----------|-----------|-----------|-------------------------------|
| | $m = 1$ | $m = 2$ | $m = 10$ | $m = 30$ | $m = 50$ | $m = 100$ | $m = 150$ | $m = 200$ | |
| 1 | 3.559 | 3.588 | 3.581 | 3.549 | 3.525 | 3.525 | 3.525 | 3.525 | 3.559 |
| 2 | 9.613 | 9.771 | 9.713 | 9.681 | 9.640 | 9.613 | 9.613 | 9.613 | 9.613 |
| 3 | 16.77 | 18.06 | 17.92 | 17.64 | 17.19 | 16.77 | 16.77 | 16.77 | 16.77 |
| 4 | 24.34 | 26.46 | 26.13 | 25.88 | 25.39 | 25.03 | 24.45 | 24.34 | 24.34 |
| 5 | 32.01 | 34.74 | 34.16 | 33.58 | 33.11 | 32.80 | 32.41 | 32.11 | 32.01 |
| 6 | 39.66 | 45.81 | 43.78 | 42.21 | 41.97 | 40.26 | 40.05 | 39.88 | 39.67 |
| 7 | 47.27 | 57.51 | 55.69 | 51.91 | 49.18 | 49.01 | 48.17 | 47.92 | 47.27 |
| 8 | 54.83 | - | 64.16 | 59.40 | 57.19 | 56.49 | 55.81 | 55.14 | 54.84 |
| 9 | 62.33 | - | 71.23 | 66.33 | 65.94 | 64.19 | 63.82 | 63.07 | 62.33 |
| 10 | 69.80 | - | 86.44 | 80.58 | 73.47 | 71.34 | 70.18 | 69.98 | 69.80 |
| 20 | 135.99 | - | 148.12 | 141.71 | 138.89 | 137.81 | 136.97 | 136.44 | 135.99 |

m = element numbers used in SEM & FEM analysis

Table 4.10: Comparison of non-dimensional natural frequencies for a symmetrical $[+15^\circ / -15^\circ / -15^\circ / +15^\circ]$ angle-ply free-free composite beam

| Mode | SEM(m) | FEM(m) | | | | | | | Chandrashekara et al. [8] |
|------|------------|------------|----------|----------|----------|-----------|-----------|-----------|------------------------------|
| | $m = 1$ | $m = 2$ | $m = 10$ | $m = 30$ | $m = 50$ | $m = 100$ | $m = 150$ | $m = 200$ | |
| 1 | 5.776 | 3.588 | 3.581 | 3.549 | 3.525 | 3.525 | 3.525 | 3.525 | 5.78 |
| 2 | 12.946 | 13.26 | 13.25 | 13.23 | 13.21 | 13.15 | 13.07 | 12.98 | 12.95 |
| 3 | 21.161 | 21.46 | 21.39 | 21.34 | 21.33 | 21.29 | 21.26 | 21.17 | 21.15 |
| 4 | 28.192 | 32.46 | 31.13 | 30.88 | 30.39 | 29.03 | 28.45 | 28.34 | 28.19 |
| 5 | 37.35 | 45.74 | 44.16 | 43.58 | 40.11 | 39.80 | 38.41 | 37.51 | 37.35 |
| 6 | 45.23 | 66.81 | 60.78 | 57.21 | 53.97 | 49.26 | 48.05 | 46.98 | 45.23 |
| 7 | 53.10 | 67.51 | 63.69 | 61.91 | 59.18 | 56.01 | 55.17 | 54.22 | 53.10 |
| 8 | 60.64 | 77.87 | 74.16 | 69.40 | 67.19 | 66.49 | 64.81 | 61.34 | 60.64 |
| 9 | 68.56 | 99.08 | 91.23 | 86.33 | 79.94 | 74.19 | 71.22 | 69.67 | 68.56 |
| 10 | 74.15 | 93.04 | 89.44 | 85.58 | 81.47 | 79.34 | 78.18 | 76.98 | 74.14 |
| 20 | 125.99 | 163.11 | 158.12 | 144.71 | 138.89 | 131.81 | 128.97 | 126.44 | 125.99 |

m = element numbers used in SEM & FEM analysis

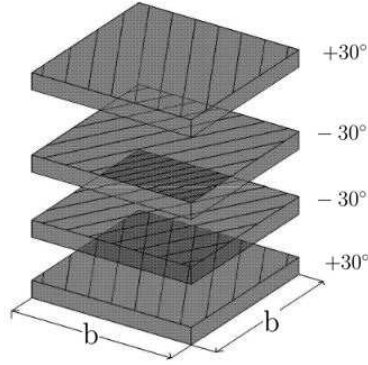


Figure 4.3: Symmetrical cross-ply orientation $[+30^\circ / -30^\circ / -30^\circ / +30^\circ]$

4.1.3 $[+30^\circ / -30^\circ / -30^\circ / +30^\circ]$ Ply Oriented Beam

Fig.(4.3) shows the orientation of the symmetrical cross-ply. Table 4.11 to 4.15 provide the comparison between present SEM model and past FEM analysis of non dimensional natural frequencies ($\bar{\omega} = \omega L^2 \sqrt{\rho / (E_1 h^2)}$) for the $[+30^\circ / -30^\circ / -30^\circ / +30^\circ]$ cross-ply symmetrical composite beams subjected to various boundary condition such as the simply-simply supported (SS) clamped-free (CF), clamped-clamped (CC) clamped-simply supported (CS) and free-free (FF) boundary condition respectively. The material properties are taken as $E_1 = 144.84 \text{ GPa}$, $E_2 = 9.65 \text{ GPa}$, $G_{12} = G_{31} = 4.14 \text{ GPa}$, $G_{23} = 3.45 \text{ GPa}$, $\nu_{12} = .3$, $\nu_{21} = 0.02$, $\rho = 1389.79 \text{ kg/m}^3$

Table 4.11: Comparison of non-dimensional natural frequencies for a symmetrical $[+30^\circ / -30^\circ / -30^\circ / +30^\circ]$ angle-ply simply supported composite beam

| Mode | SEM(m) | FEM(m) | | | | | | Chandrashekhara et al. [8] |
|------|------------|------------|----------|----------|----------|-----------|-----------|-------------------------------|
| | $m = 1$ | $m = 2$ | $m = 10$ | $m = 30$ | $m = 50$ | $m = 100$ | $m = 150$ | |
| 1 | 2.103 | 2.131 | 2.126 | 2.115 | 2.103 | 2.103 | 2.103 | 2.103 |
| 2 | 7.47 | 7.55 | 7.52 | 7.51 | 7.49 | 7.47 | 7.47 | 7.47 |
| 3 | 14.47 | 16.71 | 16.09 | 15.91 | 15.84 | 15.76 | 14.69 | 14.47 |
| 4 | 22.05 | 38.06 | 26.38 | 25.41 | 24.49 | 22.37 | 22.13 | 22.06 |
| 5 | 29.78 | 64.81 | 47.13 | 33.12 | 32.94 | 31.75 | 30.06 | 29.78 |
| 6 | 37.49 | 78.64 | 49.56 | 39.74 | 38.71 | 38.29 | 37.86 | 37.49 |
| 7 | 45.12 | - | 51.55 | 47.65 | 46.09 | 45.87 | 45.65 | 45.13 |
| 8 | 52.69 | - | 59.56 | 57.48 | 55.07 | 53.96 | 52.94 | 52.69 |
| 9 | 60.19 | - | 72.18 | 66.73 | 64.94 | 63.31 | 61.65 | 60.19 |
| 10 | 67.64 | - | 77.91 | 74.32 | 72.91 | 70.35 | 68.23 | 67.65 |
| 20 | 126.58 | - | 221.4 | 139.11 | 134.03 | 129.41 | 127.02 | 126.58 |

m = element numbers used in SEM & FEM analysis

Table 4.12: Comparison of non-dimensional natural frequencies for a symmetrical $[+30^\circ / -30^\circ / -30^\circ / +30^\circ]$ angle-ply cantilevered composite beam

| Mode | SEM(m) | FEM(m) | | | | | | Chandrashekhara et al. [8] |
|------|------------|------------|----------|----------|----------|-----------|-----------|-------------------------------|
| | $m = 1$ | $m = 2$ | $m = 10$ | $m = 30$ | $m = 50$ | $m = 100$ | $m = 150$ | |
| 1 | 0.767 | 0.771 | 0.768 | 0.767 | 0.767 | 0.767 | 0.767 | 0.767 |
| 2 | 4.27 | 4.41 | 4.35 | 4.27 | 4.27 | 4.27 | 4.27 | 4.27 |
| 3 | 10.38 | 11.69 | 11.46 | 11.13 | 11.01 | 10.38 | 10.38 | 10.38 |
| 4 | 17.48 | 38.79 | 18.84 | 18.76 | 18.72 | 17.71 | 17.48 | 17.48 |
| 5 | 25.04 | 59.85 | 26.59 | 26.38 | 26.28 | 26.11 | 25.21 | 25.04 |
| 6 | 32.71 | 73.16 | 41.56 | 39.74 | 38.69 | 35.76 | 33.03 | 32.71 |
| 7 | 40.39 | - | 51.15 | 47.85 | 44.09 | 42.87 | 40.93 | 40.39 |
| 8 | 48.01 | - | 55.65 | 54.48 | 53.01 | 52.16 | 48.93 | 48.01 |
| 9 | 55.57 | - | 66.90 | 63.83 | 61.80 | 56.93 | 55.78 | 55.57 |
| 10 | 63.07 | - | 73.90 | 71.83 | 67.18 | 65.78 | 63.78 | 63.07 |
| 20 | 127.84 | - | 151.37 | 143.84 | 131.96 | 129.42 | 128.6 | 127.84 |

m = element numbers used in SEM & FEM analysis

Table 4.13: Comparison of non-dimensional natural frequencies for a symmetrical $[+30^\circ / -30^\circ / -30^\circ / +30^\circ]$ angle-ply clamped-clamped composite beam

| Mode | SEM(m) | FEM(m) | | | | | | | Chandrashekhara et al. [8] |
|------|------------|------------|----------|----------|----------|-----------|-----------|-----------|-------------------------------|
| | $m = 1$ | $m = 2$ | $m = 10$ | $m = 30$ | $m = 50$ | $m = 100$ | $m = 150$ | $m = 200$ | |
| 1 | 4.098 | 4.101 | 4.101 | 4.098 | 4.098 | 4.098 | 4.098 | 4.098 | 4.098 |
| 2 | 16.11 | 17.91 | 17.56 | 17.26 | 16.54 | 16.11 | 16.11 | 16.11 | 16.11 |
| 3 | 30.54 | 35.18 | 34.19 | 33.09 | 32.56 | 31.90 | 31.26 | 30.63 | 30.54 |
| 4 | 45.47 | 54.21 | 51.06 | 49.79 | 47.85 | 46.03 | 45.91 | 45.58 | 45.47 |
| 5 | 60.36 | 66.91 | 66.63 | 65.08 | 64.47 | 63.88 | 62.93 | 60.99 | 60.36 |
| 6 | 75.12 | 87.05 | 85.52 | 81.96 | 80.07 | 78.89 | 77.66 | 76.59 | 75.12 |
| 7 | 89.77 | - | 103.36 | 101.73 | 98.46 | 94.13 | 91.92 | 90.88 | 89.77 |
| 8 | 104.34 | - | 109.61 | 108.39 | 107.13 | 106.22 | 105.09 | 104.89 | 104.34 |
| 9 | 118.84 | - | 123.85 | 123.56 | 122.97 | 121.06 | 120.64 | 119.94 | 118.84 |
| 10 | 126.10 | - | 139.63 | 135.14 | 130.85 | 129.50 | 128.74 | 127.02 | 126.10 |
| 20 | 248.00 | - | 267.11 | 258.86 | 255.19 | 252.91 | 250.27 | 249.84 | 248.00 |

m = element numbers used in SEM & FEM analysis

Table 4.14: Comparison of non-dimensional natural frequencies for a symmetrical $[+30^\circ / -30^\circ / -30^\circ / +30^\circ]$ angle-ply clamped-simply supported composite beam

| Mode | SEM(m) | FEM(m) | | | | | | | Chandrashekara et al. [8] |
|------|------------|------------|----------|----------|----------|-----------|-----------|-----------|------------------------------|
| | $m = 1$ | $m = 2$ | $m = 10$ | $m = 30$ | $m = 50$ | $m = 100$ | $m = 150$ | $m = 200$ | |
| 1 | 3.057 | 3.188 | 3.181 | 3.149 | 3.125 | 3.057 | 3.057 | 3.057 | 3.057 |
| 2 | 8.56 | 9.771 | 9.713 | 9.681 | 9.640 | 8.56 | 8.56 | 8.56 | 8.56 |
| 3 | 15.32 | 18.06 | 16.92 | 16.64 | 16.19 | 15.77 | 15.32 | 15.32 | 15.32 |
| 4 | 22.64 | 26.46 | 26.13 | 25.88 | 24.89 | 24.03 | 23.45 | 22.64 | 22.64 |
| 5 | 30.17 | 34.74 | 34.16 | 33.58 | 33.11 | 32.80 | 31.41 | 30.17 | 30.17 |
| 6 | 37.74 | 47.81 | 43.78 | 42.21 | 40.97 | 39.26 | 38.05 | 37.88 | 37.74 |
| 7 | 45.30 | 67.51 | 55.69 | 51.91 | 49.18 | 48.01 | 47.17 | 46.92 | 45.30 |
| 8 | 52.81 | - | 64.16 | 57.40 | 56.19 | 55.49 | 54.81 | 53.14 | 52.81 |
| 9 | 60.27 | - | 71.23 | 66.33 | 65.94 | 63.19 | 62.82 | 60.97 | 60.27 |
| 10 | 67.70 | - | 86.44 | 80.58 | 73.47 | 71.34 | 69.18 | 67.98 | 67.70 |
| 20 | 135.99 | - | 148.13 | 141.72 | 138.96 | 137.89 | 136.56 | 136.44 | 135.99 |

m = element numbers used in SEM & FEM analysis

Table 4.15: Comparison of non-dimensional natural frequencies for a symmetrical $[+30^\circ / -30^\circ / -30^\circ / +30^\circ]$ angle-ply free-free composite beam

| Mode | SEM(m) | FEM(m) | | | | | | | Chandrashekhara et al. [8] |
|------|------------|------------|----------|----------|----------|-----------|-----------|-----------|-------------------------------|
| | $m = 1$ | $m = 2$ | $m = 10$ | $m = 30$ | $m = 50$ | $m = 100$ | $m = 150$ | $m = 200$ | |
| 1 | 4.689 | 5.788 | 5.681 | 5.549 | 5.425 | 5.307 | 5.057 | 4.757 | 4.689 |
| 2 | 11.322 | 13.440 | 13.42 | 13.41 | 13.390 | 13.387 | 13.36 | 13.33 | 11.322 |
| 3 | 19.075 | 23.06 | 22.92 | 21.64 | 21.19 | 20.77 | 20.32 | 19.32 | 19.075 |
| 4 | 27.072 | 26.46 | 26.13 | 25.88 | 24.89 | 24.03 | 23.45 | 23.64 | 27.072 |
| 5 | 35.047 | 45.74 | 44.16 | 41.58 | 39.11 | 38.80 | 36.41 | 35.17 | 35.047 |
| 6 | 42.904 | 53.81 | 52.78 | 49.21 | 48.97 | 46.26 | 44.05 | 43.88 | 42.904 |
| 7 | 48.92 | 67.51 | 55.69 | 51.91 | 49.18 | 48.01 | 47.17 | 49.62 | 48.92 |
| 8 | 56.381 | 68.63 | 64.16 | 62.40 | 60.19 | 59.49 | 58.81 | 57.14 | 56.381 |
| 9 | 65.827 | 76.41 | 75.23 | 73.33 | 71.94 | 69.19 | 68.82 | 66.97 | 65.827 |
| 10 | 67.70 | 89.43 | 86.44 | 80.58 | 73.47 | 71.34 | 69.18 | 68.98 | 67.70 |
| 20 | 139.99 | 156.53 | 153.13 | 151.72 | 148.96 | 143.89 | 142.56 | 141.44 | 139.99 |

m = element numbers used in SEM & FEM analysis

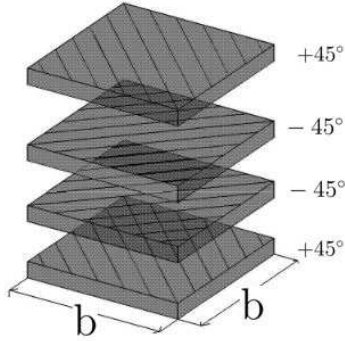


Figure 4.4: Symmetrical cross-ply orientation $[+45^\circ / -45^\circ / -45^\circ / +45^\circ]$

4.1.4 $[+45^\circ / -45^\circ / -45^\circ / +45^\circ]$ Ply Oriented Beam

Fig.(4.4) shows the orientation of the symmetrical cross-ply. Table 4.16 to 4.20 provide the comparison between present SEM model and past FEM analysis of non dimensional natural frequencies ($\bar{\omega} = \omega L^2 \sqrt{\rho / (E_1 h^2)}$) for the $[+45^\circ / -45^\circ / -45^\circ / +45^\circ]$ cross-ply symmetrical composite beams subjected to various boundary condition such as the simply-simply supported (SS) clamped-free (CF), clamped-clamped (CC), clamped-simply supported (CS) and free-free (FF) boundary condition respectively. The material properties are taken as $E_1 = 144.84 \text{ GPa}$, $E_2 = 9.65 \text{ GPa}$, $G_{12} = G_{31} = 4.14 \text{ GPa}$, $G_{23} = 3.45 \text{ GPa}$, $\nu_{12} = .3$, $\nu_{21} = 0.02$, $\rho = 1389.79 \text{ kg/m}^3$

Table 4.16: Comparison of non-dimensional natural frequencies for a symmetrical $[+45^\circ / -45^\circ / -45^\circ / +45^\circ]$ angle-ply simply supported composite beam

| Mode | SEM(m) | FEM(m) | | | | | | Chandrashekhara et al. [8] |
|------|------------|------------|----------|----------|----------|-----------|-----------|-------------------------------|
| | $m = 1$ | $m = 2$ | $m = 10$ | $m = 30$ | $m = 50$ | $m = 100$ | $m = 150$ | |
| 1 | 1.536 | 1.541 | 1.540 | 1.536 | 1.536 | 1.536 | 1.536 | 1.536 |
| 2 | 5.72 | 5.86 | 5.81 | 5.76 | 5.72 | 5.72 | 5.72 | 5.72 |
| 3 | 11.65 | 13.71 | 12.09 | 11.81 | 11.78 | 11.65 | 11.65 | 11.65 |
| 4 | 18.54 | 23.68 | 21.33 | 20.12 | 19.36 | 18.94 | 18.54 | 18.54 |
| 5 | 25.87 | 36.81 | 31.13 | 29.12 | 27.83 | 26.81 | 26.16 | 25.87 |
| 6 | 33.38 | 69.64 | 39.56 | 37.74 | 35.71 | 34.29 | 33.86 | 33.38 |
| 7 | 40.93 | - | 51.55 | 46.65 | 44.09 | 42.87 | 41.65 | 40.93 |
| 8 | 48.46 | - | 59.56 | 57.48 | 53.07 | 51.96 | 49.94 | 48.46 |
| 9 | 55.94 | - | 72.18 | 66.73 | 59.94 | 57.31 | 56.65 | 55.94 |
| 10 | 63.38 | - | 87.91 | 71.32 | 67.91 | 65.35 | 64.23 | 63.38 |
| 20 | 121.93 | - | 221.35 | 139.41 | 131.03 | 125.41 | 123.02 | 121.93 |

m = element numbers used in SEM & FEM analysis

Table 4.17: Comparison of non-dimensional natural frequencies for a symmetrical $[+45^\circ / -45^\circ / -45^\circ / +45^\circ]$ angle-ply cantilevered composite beam

| Mode | SEM(m) | FEM(m) | | | | | | Chandrashekhara et al. [8] |
|------|------------|------------|----------|----------|----------|-----------|-----------|-------------------------------|
| | $m = 1$ | $m = 2$ | $m = 10$ | $m = 30$ | $m = 50$ | $m = 100$ | $m = 150$ | |
| 1 | 0.555 | 0.561 | 0.559 | 0.557 | 0.555 | 0.555 | 0.555 | 0.555 |
| 2 | 3.24 | 3.30 | 3.28 | 3.26 | 3.24 | 3.24 | 3.24 | 3.24 |
| 3 | 8.26 | 9.02 | 8.81 | 8.66 | 8.49 | 8.26 | 8.26 | 8.26 |
| 4 | 14.51 | 18.79 | 16.84 | 15.66 | 14.93 | 14.71 | 14.58 | 14.51 |
| 5 | 21.46 | 59.85 | 29.59 | 27.38 | 25.28 | 23.11 | 22.21 | 21.46 |
| 6 | 28.75 | 72.16 | 41.16 | 39.74 | 32.69 | 30.76 | 29.03 | 28.75 |
| 7 | 36.20 | - | 51.15 | 44.85 | 39.09 | 37.87 | 36.93 | 36.20 |
| 8 | 43.70 | - | 55.63 | 54.48 | 51.01 | 47.16 | 44.09 | 43.70 |
| 9 | 51.19 | - | 66.31 | 59.74 | 56.80 | 53.93 | 52.78 | 51.19 |
| 10 | 58.64 | - | 73.90 | 67.83 | 62.18 | 60.78 | 59.78 | 58.64 |
| 20 | 121.59 | - | 149.37 | 139.84 | 128.96 | 123.42 | 122.6 | 121.59 |

m = element numbers used in SEM & FEM analysis

Table 4.18: Comparison of non-dimensional natural frequencies for a symmetrical $[+45^\circ / -45^\circ / -45^\circ / +45^\circ]$ angle-ply clamped-clamped composite beam

| Mode | SEM(m) | FEM(m) | | | | | | | Chandrashekhara et al. [8] |
|------|------------|------------|----------|----------|----------|-----------|-----------|-----------|-------------------------------|
| | $m = 1$ | $m = 2$ | $m = 10$ | $m = 30$ | $m = 50$ | $m = 100$ | $m = 150$ | $m = 200$ | |
| 1 | 3.184 | 3.199 | 3.193 | 3.186 | 3.184 | 3.184 | 3.184 | 3.184 | 3.184 |
| 2 | 13.69 | 14.91 | 14.09 | 13.86 | 13.73 | 13.69 | 13.69 | 13.69 | 13.69 |
| 3 | 27.17 | 30.18 | 29.19 | 28.09 | 27.84 | 27.31 | 27.17 | 27.17 | 27.17 |
| 4 | 41.64 | 49.21 | 46.06 | 43.79 | 42.85 | 42.03 | 41.64 | 41.64 | 41.64 |
| 5 | 56.33 | 66.91 | 64.63 | 63.08 | 59.47 | 57.88 | 56.93 | 56.33 | 56.33 |
| 6 | 70.98 | 87.05 | 85.52 | 79.96 | 76.07 | 74.89 | 72.66 | 71.68 | 70.98 |
| 7 | 85.53 | - | 106.36 | 101.73 | 98.46 | 94.13 | 91.92 | 90.88 | 85.53 |
| 8 | 99.98 | - | 113.61 | 107.39 | 105.13 | 103.22 | 101.09 | 100.03 | 99.98 |
| 9 | 114.34 | - | 127.85 | 122.13 | 121.97 | 120.06 | 118.64 | 114.98 | 114.34 |
| 10 | 121.52 | - | 139.63 | 134.14 | 129.85 | 126.50 | 124.74 | 122.02 | 121.52 |
| 20 | 220.68 | - | 247.11 | 235.86 | 229.19 | 225.91 | 223.27 | 221.84 | 220.68 |

m = element numbers used in SEM & FEM analysis

Table 4.19: Comparison of non-dimensional natural frequencies for a symmetrical $[+45^\circ / -45^\circ / -45^\circ / +45^\circ]$ angle-ply clamped-simply supported composite beam

| Mode | SEM(m) | FEM(m) | | | | | | | Chandrashekhara et al. [8] |
|------|------------|------------|----------|----------|----------|-----------|-----------|-----------|-------------------------------|
| | $m = 1$ | $m = 2$ | $m = 10$ | $m = 30$ | $m = 50$ | $m = 100$ | $m = 150$ | $m = 200$ | |
| 1 | 2.303 | 2.327 | 2.319 | 2.311 | 2.303 | 2.303 | 2.303 | 2.303 | 2.303 |
| 2 | 6.79 | 6.89 | 6.87 | 6.85 | 6.82 | 6.79 | 6.79 | 6.79 | 6.79 |
| 3 | 12.70 | 15.06 | 14.92 | 14.64 | 13.19 | 12.77 | 12.70 | 12.70 | 12.70 |
| 4 | 19.41 | 25.46 | 22.13 | 21.88 | 20.89 | 20.13 | 19.41 | 19.41 | 19.41 |
| 5 | 26.54 | 34.74 | 34.19 | 33.58 | 32.16 | 29.73 | 27.81 | 26.57 | 26.54 |
| 6 | 33.87 | 48.81 | 43.78 | 41.21 | 38.97 | 35.26 | 35.05 | 34.88 | 33.87 |
| 7 | 41.29 | 66.51 | 54.73 | 50.91 | 47.43 | 44.05 | 42.17 | 41.92 | 41.29 |
| 8 | 48.72 | - | 65.16 | 57.40 | 56.20 | 54.42 | 51.61 | 49.14 | 48.72 |
| 9 | 56.14 | - | 71.23 | 65.33 | 64.94 | 62.19 | 59.82 | 57.91 | 56.14 |
| 10 | 63.52 | - | 85.44 | 79.58 | 73.47 | 68.34 | 67.19 | 65.98 | 63.52 |
| 20 | 122.10 | - | 148.23 | 141.71 | 131.43 | 128.89 | 126.47 | 123.36 | 122.10 |

m = element numbers used in SEM & FEM analysis

Table 4.20: Comparison of non-dimensional natural frequencies for a symmetrical $[+45^\circ / -45^\circ / -45^\circ / +45^\circ]$ angle-ply free-free composite beam

| Mode | SEM(m) | FEM(m) | | | | | | | Chandrashekhara et al. [8] |
|------|------------|------------|----------|----------|----------|-----------|-----------|-----------|-------------------------------|
| | $m = 1$ | $m = 2$ | $m = 10$ | $m = 30$ | $m = 50$ | $m = 100$ | $m = 150$ | $m = 200$ | |
| 1 | 3.440 | 3.447 | 3.446 | 3.445 | 3.444 | 3.443 | 3.441 | 3.441 | 3.440 |
| 2 | 8.734 | 8.89 | 8.871 | 8.853 | 8.82 | 8.79 | 8.76 | 8.742 | 8.734 |
| 3 | 15.446 | 16.01 | 15.49 | 15.48 | 15.47 | 15.47 | 15.46 | 15.45 | 15.446 |
| 4 | 22.82 | 26.46 | 26.13 | 25.68 | 24.89 | 24.13 | 23.41 | 22.97 | 22.83 |
| 5 | 30.47 | 36.14 | 35.99 | 35.58 | 34.73 | 34.16 | 33.81 | 31.57 | 30.473 |
| 6 | 38.18 | 41.81 | 40.78 | 40.21 | 39.97 | 39.26 | 39.05 | 38.88 | 38.188 |
| 7 | 45.86 | 49.51 | 48.73 | 47.91 | 47.43 | 47.05 | 46.17 | 45.92 | 45.863 |
| 8 | 53.48 | 61.10 | 59.16 | 57.40 | 55.20 | 53.12 | 53.81 | 53.74 | 53.481 |
| 9 | 58.24 | 73.77 | 71.23 | 65.33 | 64.94 | 62.19 | 59.82 | 58.91 | 58.24 |
| 10 | 68.47 | 87.49 | 85.44 | 79.58 | 73.47 | 72.34 | 71.19 | 69.98 | 68.47 |
| 20 | 124.22 | 151.57 | 148.23 | 141.71 | 131.43 | 128.89 | 126.47 | 125.36 | 124.22 |

m = element numbers used in SEM & FEM analysis

4.2 Natural frequencies of a asymmetrical laminated composite beam with different boundary conditions

The Table 4.21 to 4.25 shows the comparison of non dimensional natural frequencies for a asymmetrical $[0^\circ/90^\circ/90^\circ/0^\circ]$ cross-ply composite beams subjected to various boundary condition such as the clamped-free (CF), clamped-clamped (CC), clamped-simply supported (CS), simply-simply supported (SS) and free-free (FF) boundary condition. They shows that FEM results converge to the SEM results as the number of finite element has increases. It is clearly visible that results of present SEM model are analogous to conventional FEM model results obtained from Chandrashekhara et al. [8]. This obtained result further present that as the number of elements used for finite element analyses is increased, the FEM results indeed converge to the present SEM results. Henceforth this will demonstrate the extremely high degree of precision of the present spectral element analysis model which can be accomplished by utilizing a minimum number of finite element component.

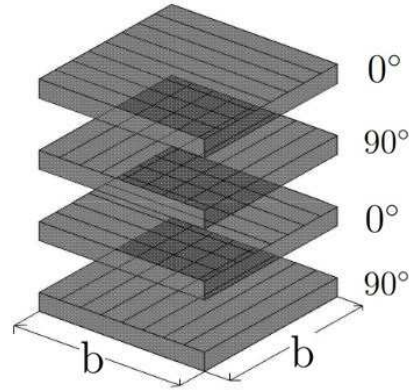


Figure 4.5: Asymmetrical cross-ply orientation $[0^\circ/90^\circ/0^\circ/90^\circ]$

4.2.1 $[0^\circ/90^\circ/0^\circ/90^\circ]$ Ply Oriented Beam

Fig.(4.5) shows the orientation of the asymmetrical cross-ply. Table 4.21 to 4.25 provide the comparison between present SEM model and past FEM analysis of non dimensional natural frequencies ($\bar{\omega} = \omega L^2 \sqrt{\rho/(E_1 h^2)}$) for the $[0^\circ/90^\circ/0^\circ/90^\circ]$ cross-ply symmetrical composite beams subjected to various boundary condition such as the simply-simply supported (SS) clamped-free (CF), clamped-clamped (CC), clamped-simply supported (CS) and free-free (FF) boundary condition respectively. The material properties are taken as $E_1 = 144.84 \text{ GPa}$, $E_2 = 9.65 \text{ GPa}$, $G_{12} = G_{31} = 4.14 \text{ GPa}$, $G_{23} = 3.45 \text{ GPa}$, $\nu_{12} = .3$, $\nu_{21} = 0.02$, $\rho = 1389.79 \text{ kg/m}^3$

Table 4.21: Comparison of non-dimensional natural frequencies for a asymmetrical $[0^\circ/90^\circ/0^\circ/90^\circ]$ angle-ply simply supported composite beam

| Mode | SEM(m) | FEM(m) | | | | | | |
|------|------------|------------|----------|----------|----------|-----------|-----------|-----------|
| | $m = 1$ | $m = 2$ | $m = 10$ | $m = 30$ | $m = 50$ | $m = 100$ | $m = 150$ | $m = 200$ |
| 1 | 1.858 | 1.901 | 1.859 | 1.858 | 1.858 | 1.858 | 1.858 | 1.858 |
| 2 | 6.723 | 8.503 | 6.761 | 6.727 | 6.727 | 6.724 | 6.723 | 6.723 |
| 3 | 13.27 | 21.95 | 13.52 | 13.30 | 13.28 | 13.28 | 13.27 | 13.27 |
| 4 | 20.55 | 38.41 | 21.38 | 20.64 | 20.58 | 20.56 | 20.54 | 20.55 |
| 5 | 28.07 | 48.06 | 30.08 | 28.29 | 28.14 | 28.08 | 28.07 | 28.07 |
| 6 | 34.30 | 76.20 | 34.43 | 34.32 | 34.31 | 34.30 | 34.30 | 34.30 |
| 7 | 35.61 | - | 36.06 | 35.93 | 35.69 | 35.63 | 35.61 | 35.61 |
| 8 | 43.13 | - | 44.28 | 44.03 | 43.69 | 43.17 | 43.14 | 43.13 |
| 9 | 50.58 | - | 51.24 | 51.13 | 50.98 | 50.86 | 50.59 | 50.58 |
| 10 | 57.99 | - | 68.38 | 59.86 | 58.66 | 58.15 | 58.07 | 58.05 |
| 20 | 115.2 | - | 183.2 | 120.6 | 115.4 | 115.2 | 115.2 | 115.2 |

m = element numbers used in SEM & FEM analysis

Table 4.22: Comparison of non-dimensional natural frequencies for a asymmetrical $[0^\circ/90^\circ/0^\circ/90^\circ]$ angle-ply cantilevered composite beam

| Mode | SEM(m) | FEM(m) | | | | | | |
|-----------------|------------|------------|----------|----------|----------|-----------|-----------|-----------|
| | $m = 1$ | $m = 2$ | $m = 10$ | $m = 30$ | $m = 50$ | $m = 100$ | $m = 150$ | $m = 200$ |
| 1 | 0.675 | 0.681 | 0.675 | 0.675 | 0.675 | 0.675 | 0.675 | 0.675 |
| 2 | 3.831 | 4.091 | 3.842 | 3.832 | 3.831 | 3.831 | 3.831 | 3.831 |
| 3 | 9.480 | 14.20 | 9.578 | 9.490 | 9.483 | 9.480 | 9.480 | 9.480 |
| 4 | 16.18 | 17.59 | 16.58 | 16.22 | 16.19 | 16.18 | 16.18 | 16.18 |
| 5 ^b | 17.27 | 42.43 | 17.30 | 17.27 | 17.27 | 17.27 | 17.27 | 17.27 |
| 6 | 23.47 | 62.30 | 24.64 | 23.60 | 23.51 | 23.48 | 23.47 | 23.47 |
| 7 | 30.92 | - | 31.02 | 31.02 | 31.01 | 30.96 | 30.92 | 30.92 |
| 8 | 35.33 | - | 35.42 | 35.40 | 35.38 | 35.37 | 35.33 | 35.33 |
| 9 | 38.42 | - | 38.50 | 38.49 | 38.46 | 38.45 | 38.42 | 38.42 |
| 10 ^b | 51.10 | - | 53.27 | 51.05 | 51.02 | 51.01 | 51.01 | 51.01 |
| 20 | 110.4 | - | 180.8 | 113.7 | 112.7 | 111.2 | 110.8 | 110.8 |

m = element numbers used in SEM & FEM analysis,

b = Axial modes

Table 4.23: Comparison of non-dimensional natural frequencies for a asymmetrical $[0^\circ/90^\circ/0^\circ/90^\circ]$ angle-ply clamped-clamped composite beam

| Mode | SEM(m) | FEM(m) | | | | | | |
|------|------------|------------|----------|----------|----------|-----------|-----------|-----------|
| | $m = 1$ | $m = 2$ | $m = 10$ | $m = 30$ | $m = 50$ | $m = 100$ | $m = 150$ | $m = 200$ |
| 1 | 3.71 | 3.78 | 3.73 | 3.73 | 3.71 | 3.71 | 3.71 | 3.71 |
| 2 | 15.06 | 15.11 | 15.09 | 15.09 | 15.08 | 15.06 | 15.06 | 15.06 |
| 3 | 28.98 | 31.56 | 29.04 | 29.03 | 29.01 | 28.98 | 28.98 | 28.98 |
| 4 | 36.25 | 38.31 | 36.29 | 36.26 | 36.26 | 36.25 | 36.25 | 36.25 |
| 5 | 50.89 | 61.39 | 50.93 | 50.91 | 50.91 | 50.90 | 50.89 | 50.89 |
| 6 | 65.47 | 66.47 | 65.50 | 65.50 | 65.49 | 65.48 | 65.47 | 65.47 |
| 7 | 72.72 | 74.62 | 72.78 | 72.77 | 72.75 | 72.73 | 72.72 | 72.72 |
| 8 | 87.12 | - | 87.29 | 87.21 | 87.13 | 87.13 | 87.12 | 87.12 |
| 9 | 98.11 | - | 98.37 | 98.23 | 98.16 | 98.12 | 98.11 | 98.11 |
| 10 | 108.5 | - | 108.43 | 108.21 | 108.13 | 108.9 | 108.6 | 108.5 |
| 20 | 200.32 | - | 200.79 | 200.67 | 200.59 | 200.44 | 200.37 | 200.32 |

m = element numbers used in SEM & FEM analysis

Table 4.24: Comparison of non-dimensional natural frequencies for a asymmetrical $[0^\circ/90^\circ/0^\circ/90^\circ]$ angle-ply clamped-simply supported composite beam

| Mode | SEM(m) | FEM(m) | | | | | | |
|------|------------|------------|----------|----------|----------|-----------|-----------|-----------|
| | $m = 1$ | $m = 2$ | $m = 10$ | $m = 30$ | $m = 50$ | $m = 100$ | $m = 150$ | $m = 200$ |
| 1 | 2.734 | 2.737 | 2.736 | 2.735 | 2.734 | 2.734 | 2.734 | 2.734 |
| 2 | 14.20 | 14.26 | 14.25 | 14.23 | 14.21 | 14.20 | 14.20 | 14.20 |
| 3 | 21.23 | 21.31 | 21.29 | 21.28 | 21.24 | 21.23 | 21.23 | 21.23 |
| 4 | 35.93 | 36.05 | 36.03 | 35.99 | 35.97 | 35.95 | 35.93 | 35.93 |
| 5 | 50.72 | 51.23 | 50.81 | 50.79 | 50.77 | 50.74 | 50.72 | 50.72 |
| 6 | 58.08 | 59.85 | 58.08 | 58.08 | 58.08 | 58.08 | 58.08 | 58.08 |
| 7 | 72.66 | 74.66 | 72.69 | 72.68 | 72.68 | 72.67 | 72.66 | 72.66 |
| 8 | 83.03 | - | 83.09 | 83.07 | 83.06 | 83.04 | 83.04 | 83.03 |
| 9 | 94.26 | - | 94.39 | 94.37 | 94.33 | 94.31 | 94.29 | 94.26 |
| 10 | 108.54 | - | 108.62 | 108.59 | 108.57 | 108.55 | 108.53 | 108.54 |
| 20 | 193.32 | - | 194.09 | 193.43 | 193.39 | 193.35 | 193.33 | 193.32 |

m = element numbers used in SEM & FEM analysis

Table 4.25: Comparison of non-dimensional natural frequencies for a asymmetrical $[0^\circ/90^\circ/0^\circ/90^\circ]$ angle-ply free-free composite beam

| Mode | SEM(m) | FEM(m) | | | | | | |
|------|------------|------------|----------|----------|----------|-----------|-----------|-----------|
| | $m = 1$ | $m = 2$ | $m = 10$ | $m = 30$ | $m = 50$ | $m = 100$ | $m = 150$ | $m = 200$ |
| 1 | 4.145 | 4.147 | 4.147 | 4.146 | 4.146 | 4.145 | 4.145 | 4.145 |
| 2 | 17.50 | 17.56 | 17.55 | 17.53 | 17.53 | 17.52 | 17.50 | 17.50 |
| 3 | 32.807 | 33.01 | 32.89 | 32.86 | 32.85 | 32.83 | 32.80 | 32.807 |
| 4 | 40.713 | 41.63 | 41.58 | 41.35 | 41.07 | 40.94 | 40.76 | 40.713 |
| 5 | 55.81 | 56.83 | 55.41 | 56.04 | 55.97 | 55.93 | 55.88 | 55.81 |
| 6 | 67.19 | 71.01 | 70.27 | 69.23 | 68.65 | 68.08 | 67.29 | 67.19 |
| 7 | 77.90 | 83.54 | 82.04 | 81.13 | 80.68 | 79.67 | 78.66 | 77.90 |
| 8 | 92.02 | - | 99.09 | 97.07 | 96.45 | 96.44 | 94.24 | 92.02 |
| 9 | 99.264 | - | 108.82 | 105.37 | 103.33 | 101.31 | 100.29 | 99.264 |
| 10 | 111.84 | - | 119.59 | 118.38 | 116.72 | 114.15 | 112.53 | 111.84 |
| 20 | 189.32 | - | 197.09 | 195.43 | 193.39 | 191.35 | 190.33 | 189.32 |

m = element numbers used in SEM & FEM analysis

4.3 Effect of Coupling Rigidity and Axial Force on dispersion curve

Effect of coupling rigidity K and axial force P on dispersion curve can be presented graphically, and it is clearly visible that as the coupling rigidity K tends to decrease the group velocity of the axial mode at all frequency while, increase the group velocity of the shear mode after the cut-off frequency.

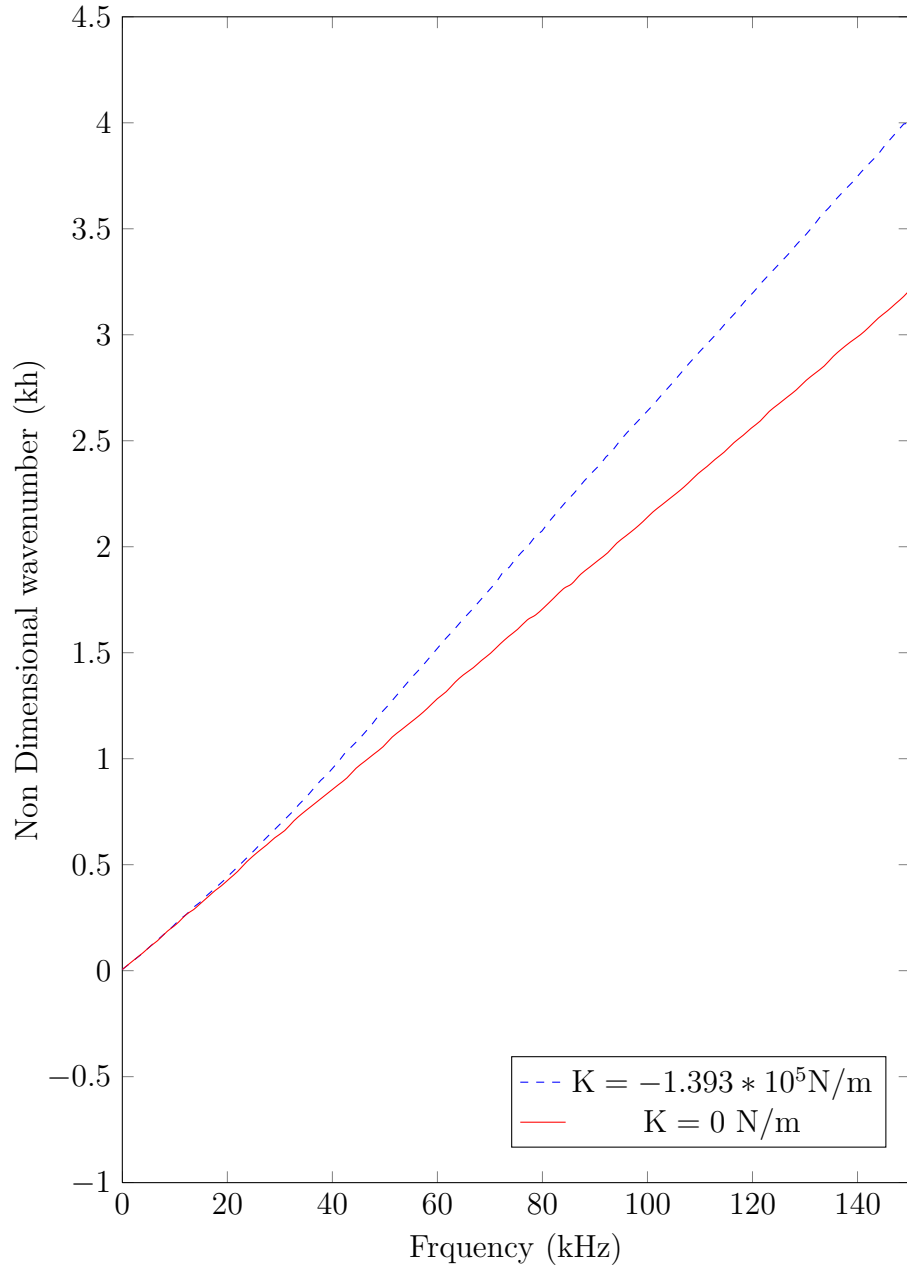


Figure 4.6: Variation of Non-Dimensional Natural Frequency in dispersion curve with varying coupling rigidity K in axial mode

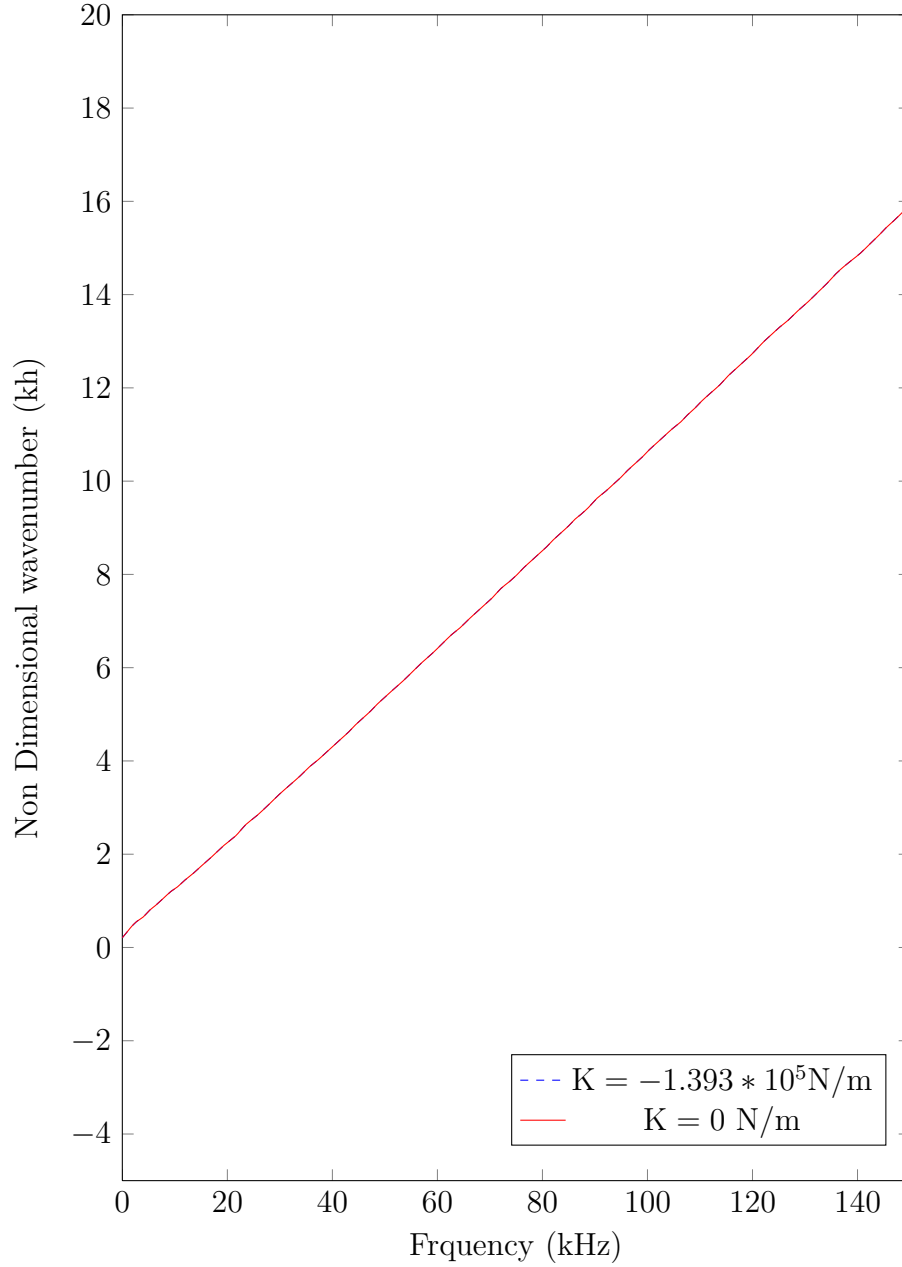


Figure 4.7: Variation of Non-Dimensional Natural Frequency in dispersion curve with varying coupling rigidity K in bending mode

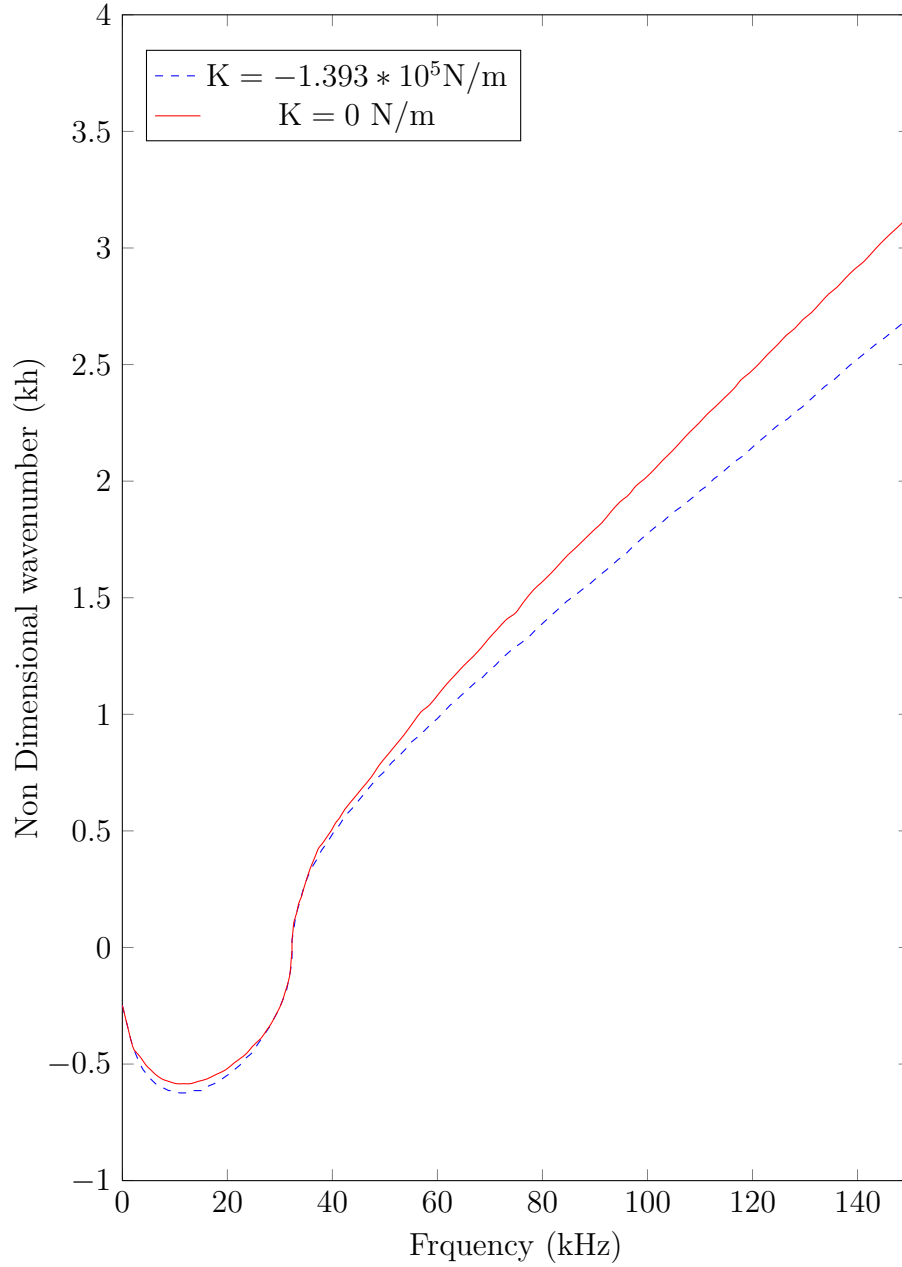


Figure 4.8: Variation of Non-Dimensional Natural Frequency in dispersion curve with varying coupling rigidity K in shear mode

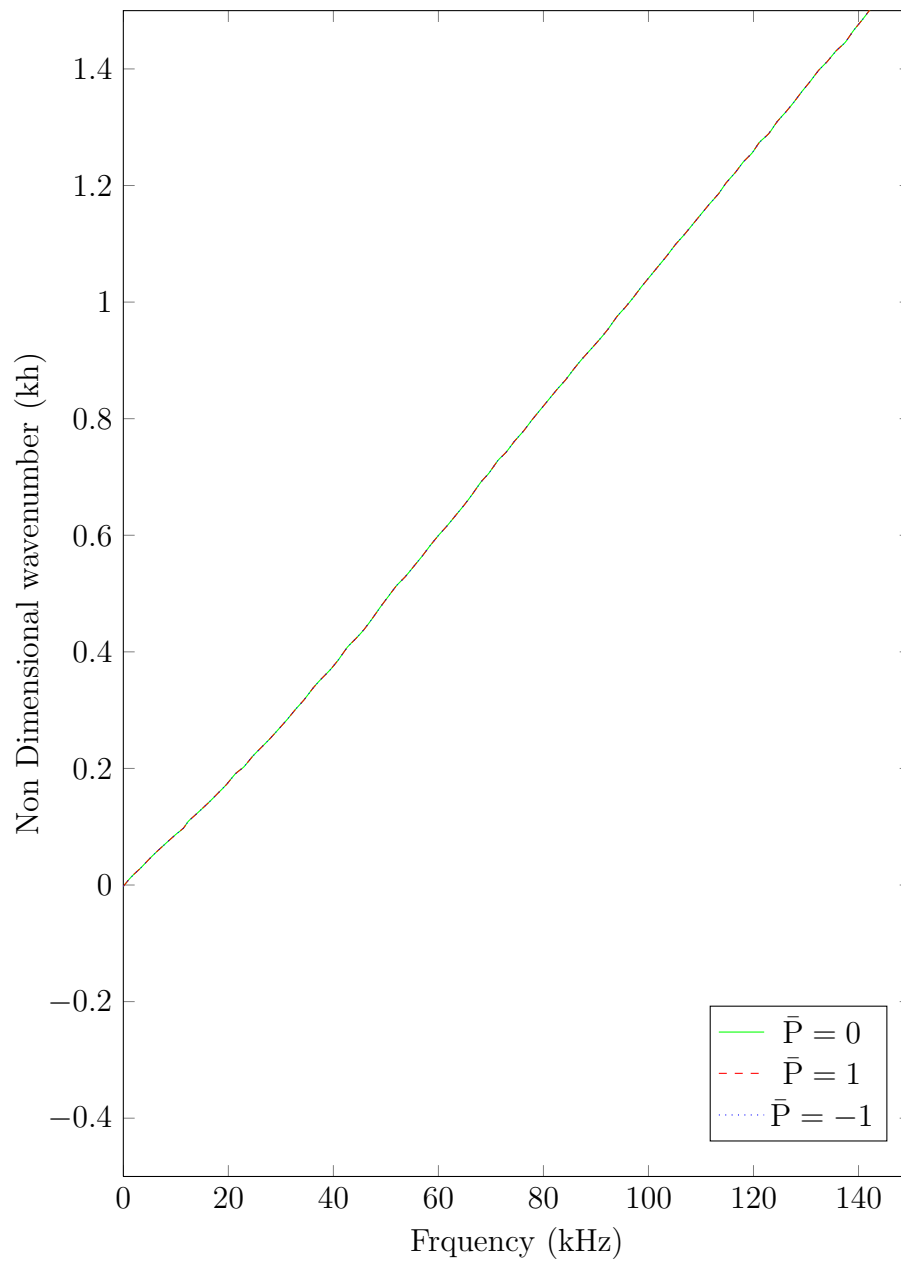


Figure 4.9: Variation of Non-Dimensional Natural Frequency in dispersion curve with varying axial loading P in axial mode

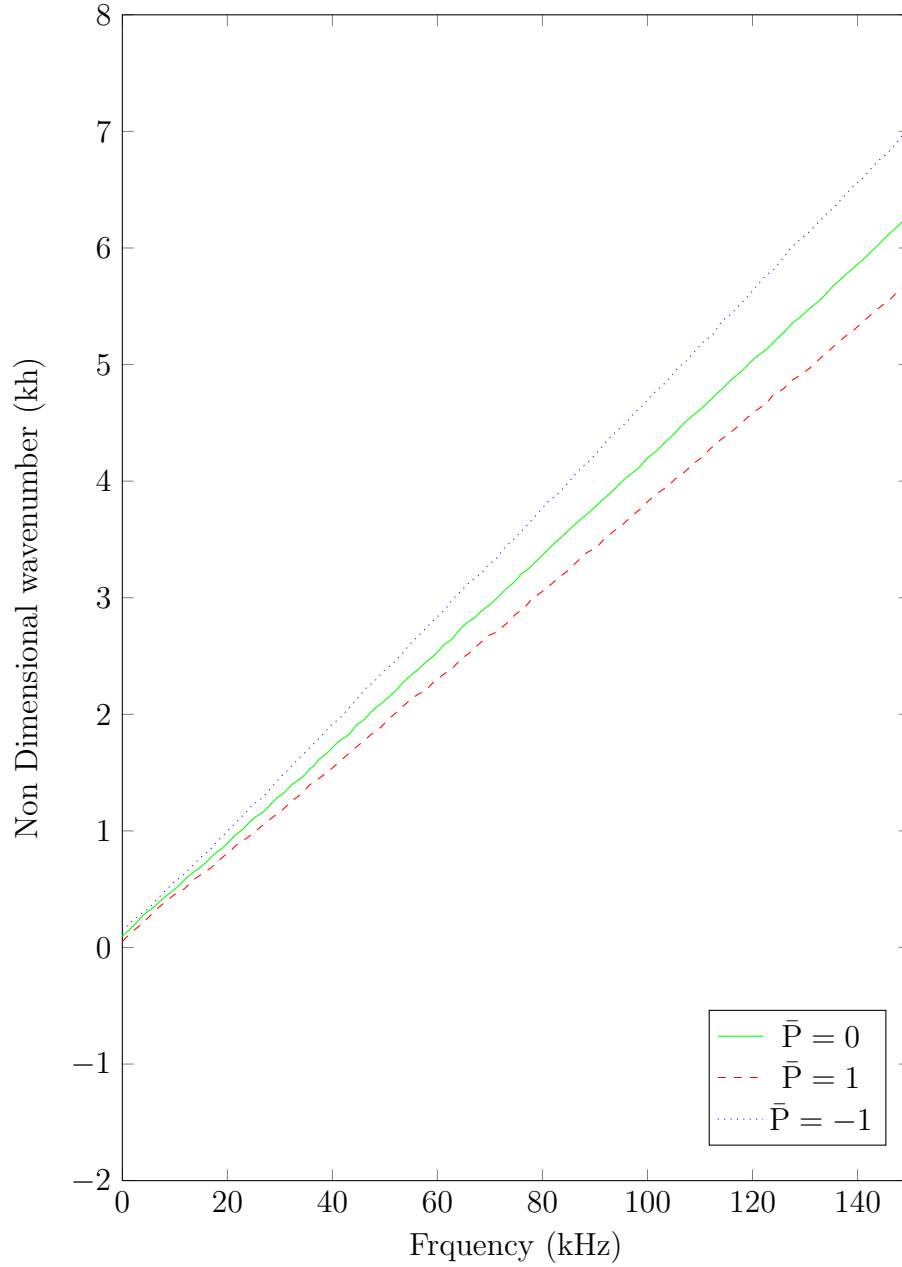


Figure 4.10: Variation of Non-Dimensional Natural Frequency in dispersion curve with varying axial loading P in bending mode

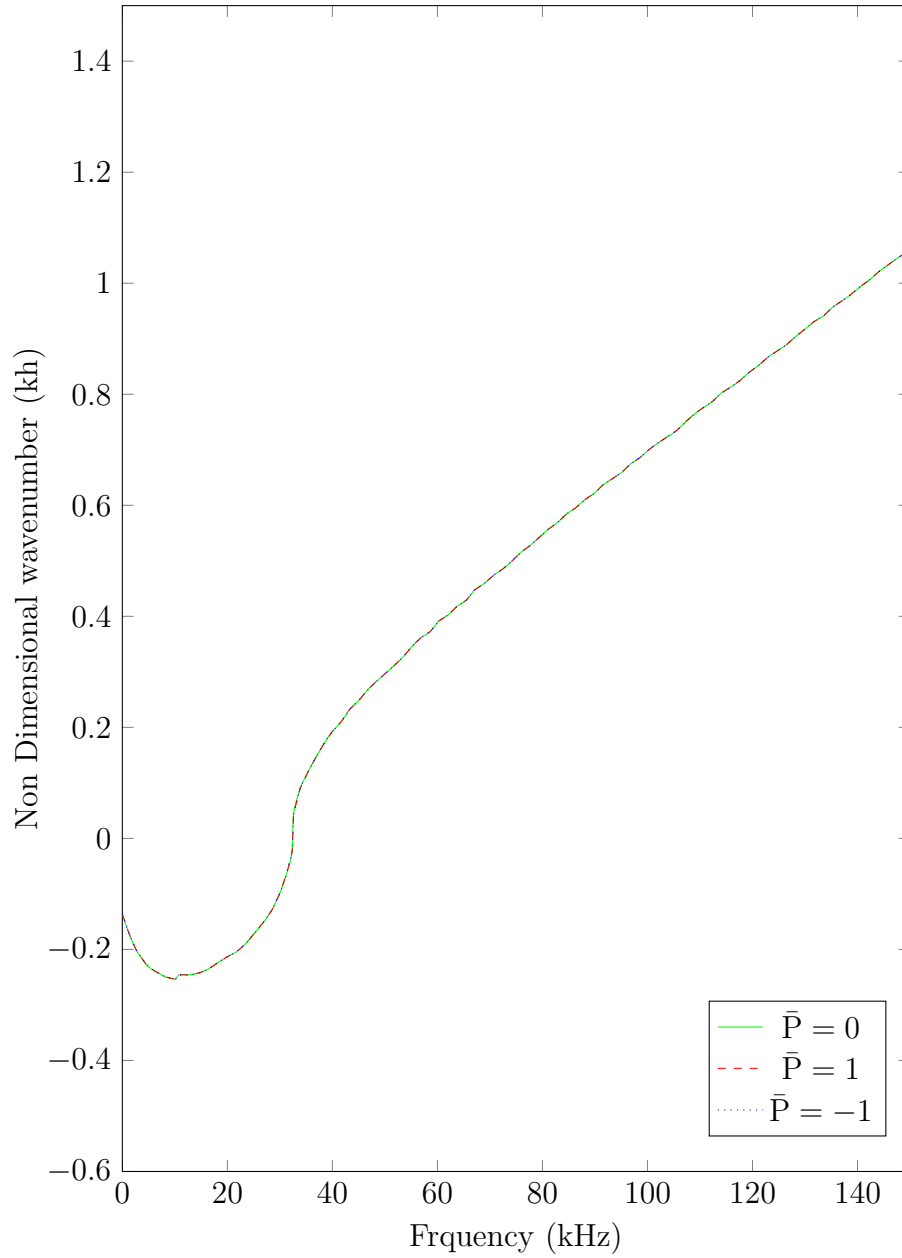


Figure 4.11: Variation of Non-Dimensional Natural Frequency in dispersion curve with varying axial loading P in shear mode

Chapter 5

Conclusion

In this study the Spectral Element model is presented for the axial-bending-shear coupled vibration analysis of both symmetrical as well as asymmetrical laminated composite Timoshenko beam subjected to axial loading. This spectral element model is formulated using the frequency dependent dynamic shape function with the help of generalised frequency domain governing equation of motion. The nondimensional natural frequencies obtained for the beams with various boundary condition are compared with the published ones. The following conclusion may be arrived as:

1. The present SEM model is capable of high precision vibration analysis with minimum number of degrees of freedom and computational cost. By numerical examination the extremely high precision of present SEM model is verified.
2. With the increase of compressive axial loading the fundamental natural frequencies of composite beam tends to decrease.
3. This spectral element method (SEM) is easy to implement as it is similar to the conventional Finite Element Method (FEM).

4. The effect of the coupling rigidity K and the axial force P on the dispersion curve are studied and presented graphically.
5. With the increase of natural frequencies, the non-dimensional wavenumber increases at greater rate when coupling rigidity is considered for axial mode but for shear mode, the non dimensional wavenumber increases at slower rate when coupling rigidity is considered.
6. With the change in the axial loading, the non-dimensional wavenumber does not change for axial and shear mode i.e. its value remains constant.

Chapter 6

Future scope of study

The free vibration analysis of axial-flexural-shear coupled beams with un-damped condition has been studied with the help of spectral element method and the result obtained are in excellent agreement proving the efficiency of the SEM analysis. Thus making the following possible extensions which can be made in the future studies.

1. Axial-flexural-shear coupled vibration analysis can be done for curved beams with various boundary conditions.
2. The frequency parameter and different wave-mode for varying cross-section of the beams can be done for both damped and un-damped vibration.
3. The spectral element method can be employed for the dynamic analysis of more complex structures.
4. Time history analysis can be performed.
5. The spectral element method can be applied for smart structures.

Bibliography

- [1] Banerjee JR. Dynamic stiffness formulation for structural elements: a general approach. *Computers and Structures*, 63:101–103, 1997.
- [2] Leung AYT. *Dynamic Stiffness and Substructures*, Springer-Verlag. London, 1993.
- [3] Narayanan GV and Beskos DE. Use of dynamic influence coefficients in forced vibration problems with the aid of fast fourier transform. *Computers and Structures*, 9(2):145–150, 1978.
- [4] Gopalakrishnan S and Mahapatra DR. Spectral-element-based solution for wave propagation analysis of multiply connected unsymmetric laminated composite beams. *Journal of Sound and Vibration*, 237:819–836, 2000.
- [5] Sierakowski RL and Vinson JR. *The behavior of structures composed of composite materials*. The Netherlands: Martinus Nijhoff, 1986.
- [6] Yang TY and Chen AT. Static and dynamic formulation of symmetrically laminated beam finite element for a microcomputer. *Journal of Composite Materials*, 19:459–475, 1985.
- [7] Abramovitch H. Shear deformation and rotary inertia effects of vibrating composite beams. *Composite Structures*, 20:165–173, 1992.
- [8] Chandrashekhara K, Krishnamurthy K, and Roy S. Free vibration of composite beams including rotary inertia and shear deformation. *Composite Structures*, 14:269–279, 1990.
- [9] Dong XJ, Meng G, Li HG, and Ye L. Vibration analysis of a stepped laminated composite timoshenko beam. *Mech Res Commun*, 32:572–581, 2005.
- [10] Palacz M, Krawczuk M, and Ostachowicz W. The spectral finite element model for analysis of flexural-shear coupled wave propagation. part 1: Laminated multilayer composite beam. *Composite Structures*, 68:37–44, 2005.

- [11] Teoh LS and Huang C-C. The vibration of beams of fibre reinforced material. *Journal of Sound and Vibration*, 51(4):467–473, 1977.
- [12] Krishnaswamy S, Chandrashekhara K, and Wu WZB. Analytical solutions to vibration of generally layered composite beams. *Journal of Sound and Vibration*, 159(1):85–99, 1992.
- [13] Abramovich H and Livshits A. Free vibrations of non-symmetric cross-ply laminated composite beams. *Journal of Sound and Vibration*, 176(5):597–612, 1994.
- [14] Eisenberger M, Abramovich H, and Shulepov O. Dynamic stiffness analysis of laminated beams using a first order shear deformation theory. *Composite Structures*, 31(4):265–271, 1995.
- [15] Hassan GA, Aly MF, and Goda I. The effects of fibre orientation and laminate stacking sequence on the torsional natural frequencies of laminated composite beams. *Journal of Research in Engineering and Technology*, 2(12):2319–2321, 2013.
- [16] Teboub Y and Hajela P. Free vibration of generally layered composite beams using symbolic computational. *Composite Structures*, 33(3):123–134, 1995.
- [17] Bannerjee JR and Williams FW. Exact dynamic stiffness matrix for composite timoshenko beams with applications. *Journal of Sound and Vibration*, 194(4):573–585, 1996.
- [18] Lam KY and Sathiyamoorthy TS. Low-velocity impact response for laminated stepped beam. *Composite Structures*, 35(4):343–355, 1996.
- [19] Banerjee JR. Free vibration of axially loaded composite timoshenko beams using the dynamic stiffness matrix method. *Computers and Structures*, 69(2):197–208, 1998.
- [20] Shi G and Lam KY. Finite element vibration analysis of composite beams based on higher-order beam theory. *Journal of Sound and Vibration*, 219(4):707–721, 1999.
- [21] Bassiouni AS, Gad-Elrab RM, and Elmahdy TH. Dynamic analysis for laminated composite beams. *Composite Structures*, 44(2):81–87, 1999.
- [22] Mahapatra DR and Gopalakrishnan S. A spectral finite element model for analysis of axial-flexural-shear coupled wave propagation in laminate composite beams. *Composite Structures*, 59:67–88, 2003.
- [23] Chakraborty A, Mahapatra DR, and Gopalakrishnan S. Finite element analysis of free vibration and wave propagation in asymmetric composite beams with structural discontinuities. *Composite Structures*, 55:23–36, 2002.

- [24] Ruotolo RA. Spectral element for laminated composite beams: theory and application to pyroshock analysis. *Journal of Sound and Vibration*, 270:149–169, 2004.
- [25] Banerjee JR. Dynamic stiffness formulation for structural elements: a general approach. *Computers and Structures*, 63:101–103, 1997.
- [26] Doyle JF. *Wave propagation in structures: spectral analysis using fast discrete Fourier transforms*. New York: Springer-Verlag, 1997.
- [27] Lee U. *Spectral element method in structural dynamics*. John Wiley & Sons, 2009.
- [28] Li J, Shen R, Hua H, and Jin X. Bending-torsional coupled dynamic response of axially loaded composite timoshenko thin-walled beam with closed cross-section. *Composite Structures*, 64(1):23–25, 2004.
- [29] Reddy JN. *Mechanics of laminated composite plates: theory and analysis*. New York: CRC Press, 1997.
- [30] Abramovitch H. Shear deformation and rotary inertia effects of vibrating composite beams. *Composite Structures*, 20:165–173, 1992.